

Using Pulsed Gradient Spin Echo NMR for Chemical Mixture Analysis: How to Obtain Optimum Results

BRIAN ANTALEK

Imaging Materials and Media Research and Development, Eastman Kodak Company, Rochester, New York 14650-2132

ABSTRACT: Pulsed gradient spin echo NMR is a powerful technique for measuring diffusion coefficients. When coupled with appropriate data processing schemes, the technique becomes an exceptionally valuable tool for mixture analysis, the separation of which is based on the molecular size. Extremely fine differentiation may be possible in the diffusion dimension but only with high-quality data. For fully resolved resonances, components with diffusion coefficients that differ by less than 2% may be distinguished in mixtures. For highly overlapped resonances, the resolved spectra of pure components with diffusion coefficients that differ by less than 30% may be obtained. In order to achieve the best possible data quality one must be aware of the primary sources of artifacts and incorporate the necessary means to alleviate them. The origin of these artifacts are described, along with the methods necessary to observe them. Practical solutions are presented. Examples are shown that demonstrate the effects of the artifacts on the acquired data set. Many mixture analysis problems may be addressed with conventional high resolution pulsed field gradient probe technology delivering less than 0.5 T m^{-1} (50 G cm^{-1}). © 2002 Wiley Periodicals, Inc. Concepts Magn Reson 14: 225–258, 2002

KEY WORDS: pulsed gradient spin echo NMR; diffusion; mixture analysis; diffusion ordered spectroscopy; direct exponential curve resolution algorithm; chemometrics

Received 9 July 2001; revised 17 January 2002; accepted 23 January 2002

Correspondence to: B. Antalek; E-mail: brian.antalek@kodak.com.

Concepts in Magnetic Resonance, Vol. 14(4) 225–258 (2002)

Published online in Wiley InterScience (www.interscience.wiley.com). DOI 10.1002/cmr.10026

© 2002 Wiley Periodicals, Inc.

INTRODUCTION

Mixture analysis continues to be one of the most challenging pursuits in analytical science. For solution problems, high performance liquid chromatography (HPLC) stands as the premier method for physical component separation. However, it lacks the ability to provide detailed structural information. For

this reason it is often used in tandem with mass spectrometry (MS) or even NMR to form powerful techniques (LC-MS, LC-NMR). Some groups even combined all three to form LC-MS-NMR (1–5). Although these techniques are very powerful, they are difficult and expensive to implement.

One technique that is gaining popularity and that can be used as a facile first experiment to screen and characterize a mixture is called pulsed gradient spin echo (PGSE) NMR. This technique relies on differences in diffusion coefficients (and therefore differences in the molecular size) as a means to separate components in a solution mixture. It requires no special sample preparation or chromatographic method optimization, it may be performed with standard NMR equipment, and it can be as easy to execute as a standard 2-dimensional (2-D) NMR experiment. Several reviews are available (6–9).

Originally utilized as a technique to measure diffusion coefficients of components in solution (10, 11) and to define domain size in emulsions (12, 13) in the late 1960s and early 1970s, PGSE NMR became more popular as instrumentation was developed and spectral resolution improved. The idea of using PGSE NMR for mixture analysis was suggested in the early 1980s (14). Despite this, it was not until shielded gradients and stable gradient drivers became commercially available in the early 1990s that the method gained widespread use. Furthermore, the studies generally focused on the analysis of known compounds in mixtures, not on the characterization of unknowns.

Johnson and coworkers developed a formal method for using the PGSE NMR experiment for mixture analysis. The data processing approach, which they called diffusion ordered spectroscopy (DOSY) (15–17), results in a 2-D plot with a chemical shift in one dimension and a diffusion coefficient in the other. DOSY is an extremely useful data processing scheme because it enables one to quickly correlate resonances with a specific component in solution, rather than a specific spin system. It is actually used to describe a number of different processing schemes that result in such a 2-D plot. These will be briefly discussed in the article. Other methods to process the PGSE NMR data have recently emerged that produce a rather different display of results, and they have some advantages compared to the DOSY analysis. These curve resolution methods mathematically resolve the spectra of the individual components, along with their associated diffusion coefficients. They include the direct exponential curve resolution algorithm (DECRA) (18–20), component resolved (CORE) (21–23), and multivariate curve resolution (MCR) (24).

There are several recent examples of the use of PGSE NMR for mixture analysis including studies of small molecules (22, 25–30), polymer mixtures (20, 21, 24, 31–33), and quick screening methods for bioactivity (34–38). Mixture analysis in the solid state was recently reported (39) utilizing spin diffusion and ^{13}C T_1 differences instead of translational diffusion.

The ideal mixture analysis delivers extreme accuracy and precision in the diffusion dimension, even in the presence of severe spectral overlap. This is difficult to achieve. The quality of the final result, and the concomitant information content of that result, relies on both the quality of the acquired raw data and the proper choice of data processing methods. Several complications may occur during the acquisition process that will degrade the quality of the data and limit the capabilities of the technique. This is especially true for cases where separation based on fine differences in the molecular size (and therefore differences in diffusion coefficients) is necessary or where automation is important. These problems stem from the probe design; hence, the degree may vary substantially. After fully characterizing these problems they may be managed effectively with the proper pulse sequence elements and appropriate sample configurations. The methods for data analysis differ widely and can produce varied results. For example, some DOSY methods can provide very fine differentiation in the diffusion dimension but only for fully resolved resonances. On the other hand, DECRA (and yet other DOSY methods) can resolve overlapped regions but at the expense of resolution in the diffusion dimension. Therefore, a combination of analysis methods may be needed to fully characterize the mixture.

The purpose of this article is twofold: to describe how to optimize the acquisition process of the PGSE NMR experiment to obtain high quality data and to describe various approaches to analyze the data so that the information obtained from the mixture analysis can be maximized. Simple methods for characterizing data artifacts are described, along with several strategies for improvement. Two primary approaches to the data analysis are discussed in light of what is currently considered state of the art. Three questions will be answered. How different in size must two components be in order for PGSE NMR to be useful as a means of separation? How many components may be separated in one experiment? What is the upper molecular size limit? After brief theoretical and experimental sections the data quality and necessary elements for proper data acquisition are described. The final sections elucidate the data analysis process with several examples. The scope of this article is restricted to mixture analysis of relatively

low molecular weight solution components in nonviscous solutions undergoing free (unobstructed or unrestricted) diffusion. Issues relating to restricted diffusion or diffusion in heterogeneous media are thoroughly treated elsewhere (9, 40). Furthermore, a thorough treatment of the relationship between the signal attenuation in the PGSE NMR experiment and diffusion is not presented because it was described previously (8, 9).

THEORETICAL SYNOPSIS

Diffusion

Molecules in solution are in constant motion and experience both rotational and translational motion. The process of translational motion in solution is commonly referred to as self-diffusion and is defined with a self-diffusion coefficient D ($\text{m}^2 \text{s}^{-1}$). The value of D may be approximated by the Stokes–Einstein equation:

$$D = kT/6\pi\eta R_H \quad [1]$$

where k (J K^{-1}) is the Boltzmann constant, T is the temperature (K), η (P) is the solvent viscosity, and R_H (m) is the hydrodynamic radius. The relationship is strictly valid for a spherical particle with a radius R_H , but it may be used to estimate the size of molecules in solution. The distance a molecule will travel in a single direction during a defined amount of time t (s) is given by (6)

$$z = (2Dt)^{1/2} \quad [2]$$

Of course, not every molecule will travel the distance defined in Eq. [2] during a specific time period. This is why z (m) is often referred to as a root mean square (RMS) distance and it represents an ensemble average of many particles. In the case of unrestricted diffusion a conditional probability function was derived (6),

$$P_s(z, t) = (4\pi Dt)^{-1/2} \exp[-(z - v_z t)^2/4Dt] \quad [3]$$

that describes the average probability for any particle to have a dynamic displacement z over a time t . The variable v_z (m s^{-1}) is the velocity of the particle, and the term is included to illustrate that velocity and diffusion are two separate matters and may be separately analyzed. This function is illustrated in Fig. 1. Two populations of molecules are represented, each having its own characteristic diffusion coefficient. After some time t the probabilities of finding the

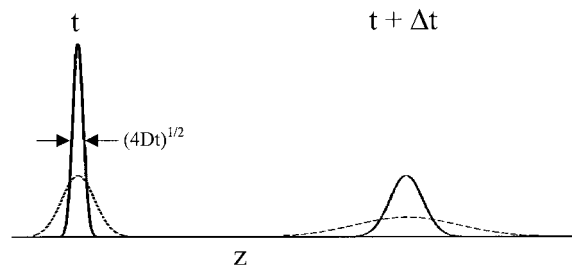


Figure 1 Probability curves derived from the average propagator function (Eq. [3]) for two populations of molecules and in one dimension. The diffusion coefficient for the molecules represented by the dashed line is greater than that represented by the solid line. A velocity component is superimposed upon the diffusion component.

particles along a single dimension are represented as normalized Gaussian curves. After time passes, $t + \Delta t$, the curves broaden. Because a velocity term is included, the curves shift to the right after Δt . In a typical PGSE NMR experiment, any velocity component, brought about by convection, for example, should be strictly avoided or properly compensated.

In order to measure true translational motion, enough time must be allowed to pass in the experiment for z to be several times larger than R_H . This point is particularly important for large molecules such as polymers. If the amount of time used is too short, we may actually measure the translation of a chain segment or the rotational diffusion rather than the translational diffusion.

PGSE NMR

PGSE NMR is a method devised by Stejskal and Tanner (10), and it is derived from the nuclear spin echo concept of Hahn (41) and Carr and Purcell (42). Two magnetic field gradient pulses are used in the experiment, and they are essential for interrogating the effects of translational motion on the signal intensity. A thorough description of the experiment is given by Price (9), but a brief qualitative discussion of the effect of the magnetic field gradient is in order. It is assumed that a modern instrument with a vertical-bore magnet is used. The magnetic field gradient is typically produced by an anti-Helmholtz coil (Maxwell pair) geometry consisting of two coils of wire connected in series and positioned coaxially outside the radio frequency (RF) coil. One gradient coil is positioned above the RF coil and carries current in one direction while the other gradient coil is positioned below the RF coil and carries current in the opposite direction. The magnetic field that is produced by the gradient coils creates a situation where

the magnetic field strength is added to the top of the sample volume and subtracted from the bottom, or vice versa. Along the length of the sample during the gradient pulse there is a uniformly changing magnetic field.

There are several features that are designed into the gradient coils, two of which are very important: shielding and field linearity. A magnetic field is not only produced within the gradient coils but also produced outside as well. Whenever an electrically conducting material (i.e., the probe body) experiences a changing magnetic field, such as at the beginning or end of a gradient pulse, an electrical current (eddy current) is set up in nearby conducting surfaces (i.e., the probe body), creating a secondary field that opposes the change. This is problematic because the secondary field interferes with the acquisition of the free induction decay (FID). A modern coil design is actively shielded to minimize this. That is, it includes several coils of wire placed around and in series with the two main coils in such a way as to create an equal but opposite field outside the main coils. Therefore, the field created by shielding the gradient coils cancels that produced by the main coils at the probe body. The other design criterion is gradient field uniformity. The applied gradient must be constant (uniform) along the z direction (i.e., along the long dimension of the NMR tube). That is, a constant change in the magnetic field exists at all points in the z direction. The magnetic field changes *linearly*, but the gradient is *constant (uniform)*. The reason that a nonuniform gradient field is problematic will soon be apparent.

Equation [4] describes the effect of the gradient on the Larmor frequency, ω_z (rad s⁻¹).

$$\omega_z = \gamma B_0 + \gamma g_z z \quad [4]$$

where B_0 (T) is the main field oriented in the z direction, g_z (T m⁻¹) is the gradient applied in the z direction, z (m) is the position of the spin (nucleus of interest), and γ is the gyromagnetic ratio (rad T⁻¹ s⁻¹). Equation [5] describes the induced position-dependent phase angle of the spins, φ_z (rad),

$$\varphi_z = \delta \gamma g_z z \quad [5]$$

where δ (s) is the time duration of the applied gradient pulse. Equation [4] excludes the shielding term and Eqs. [4] and [5] are true for a single quantum coherence.

The essential process for obtaining signal discrimination based on translational displacement is illustrated in Fig. 2(a). During excitation the net magnetization is instantaneously placed in the xy plane and

the phase of the spins is coherent. After excitation a gradient pulse encodes the spins. The word encode in this context means that the gradient actually labels the position of the spins by producing a spatially dependent phase angle, defined by Eq. [5]. In other words, the Larmor frequency varies uniformly along the z direction during the gradient pulse. Each plane of the sample perpendicular to the z direction contains spins that will be affected by the gradient pulse in exactly the same way. One way to think about this process is to visualize a twist in a piece of taut string. The higher the gradient strength and the longer the gradient pulse, the more twisted the string becomes. During the gradient, along the z direction, the direction of the spins assume a regular helix or twist whose periodicity is defined by $2\pi z/\varphi_z$. The system then evolves. Two things happen during the evolution period: because the spins are always undergoing random translational motion in solution, the extent of which defined by the self-diffusion coefficient, some will change position along the z direction; and the spin magnetization is rotated 180° by a single RF pulse (or a series of RF pulses). After the evolution period the spin position is decoded with an identical gradient pulse. Because the 180° pulse (or series of pulses) was applied, the sign of the spin phase angle is reversed and the phase contribution added to the spins by the first gradient pulse is subtracted by the second. If no diffusion took place, the maximum signal is obtained. (We have not yet considered relaxation.) However, if diffusion took place, some spins would not be in the same position along the z axis during the second gradient pulse as during the first. Therefore, their phase component imposed by the first gradient would not be cancelled by the second gradient and the signal would be diminished. It is important that the gradient be constant for the entire excited region so that the same gradient strength is experienced no matter where the spin is.

The basic PGSE pulse sequence is illustrated in Fig. 2(b). The two identical gradient pulses are used on both sides of a 180° pulse. The equation that is derived to represent the signal intensity generated by the pulse sequence in Fig. 2(b) is given below (10).

$$E_{(t=2\tau_2)} = E_{(t=0)} \exp[-D\gamma^2 g^2 \delta^2 (\Delta - \delta/3) - R] \quad [6]$$

where $g = g_z$, E is the measured signal intensity, Δ (s) is the time between the two gradients in the pulse sequence (and hence defines the time for which diffusion is observed), and R is a constant that takes nuclear relaxation into account. For the spin echo pulse sequence [Fig. 2(b)], $R = 2\tau_2/T_2$. The gradient pulses must also be exactly the same in both strength and length.

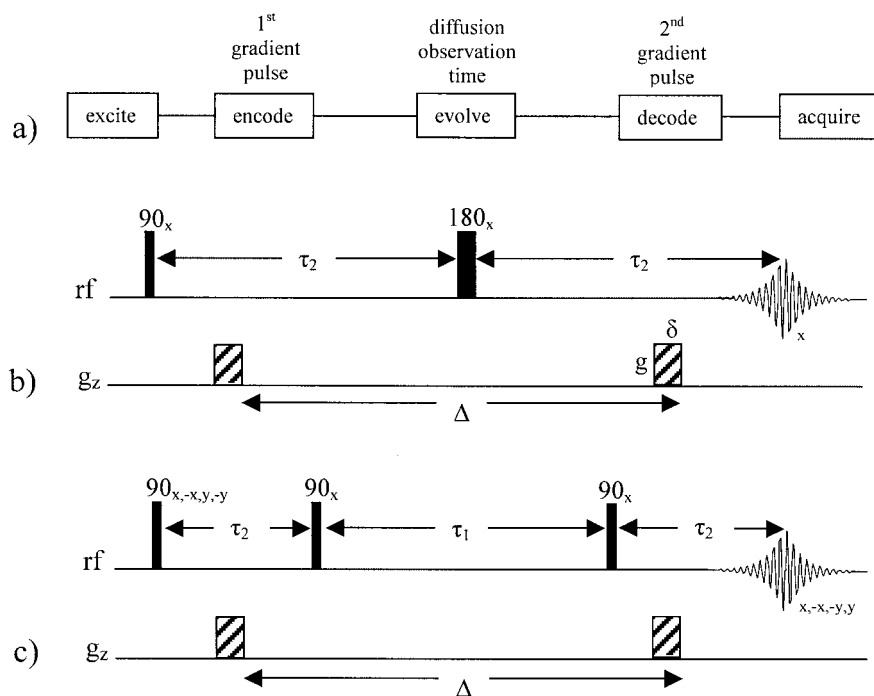


Figure 2 (a) The essential components of a PGSE NMR diffusion experiment include, besides an excitation and acquisition process, three key elements: an encoding element performed by a gradient pulse that labels the position of the spins with a position-dependent phase angle, an evolution period long enough to allow for sufficient translational displacement of the spins to occur, and a decoding element performed by a gradient pulse identical to the first that refocuses those spins that have not changed position during evolution. (b) The PGSE pulse sequence. (c) The pulsed gradient stimulated echo pulse sequence.

The experiment is typically performed by varying the gradient strength g for several values and collecting the FIDs, although δ or Δ may also be varied to give signal attenuation. The former is the preferred method for mixture analysis because it easily allows for the pulse sequence timing to be constant throughout the experiment. A Fourier transformed data set contains families of resonances with common decay behavior. All of the resonances that belong to a pure component in the mixture will decay exponentially at the same rate with respect to the square of the gradient area $(g\delta)^2$. The resonances are then differentiated based upon this decay rate.

There are potentially severe problems with the spin echo version of the PGSE NMR experiment. The magnetization evolves entirely in the xy plane. Whereas the spins undergo relaxation because of T_2 processes, the signal will decay rapidly for macromolecules. Furthermore, J -modulation effects can degrade the quality of the final spectrum. Because the signal for coupled spins modulates in the xy plane, the final spectrum may contain peaks with negative intensity and/or have phase components different from

the others. Although J modulation is well understood and is a natural consequence of the delays in the pulse sequence, the final spectrum may look very different from a standard spectrum and may be difficult to interpret or process using DOSY or other methods. For mixture analysis the effects of J modulation are generally considered a nuisance and should be minimized. In order to understand how it works, let us assume we have the case of two coupled hydrogen nuclei within an AX spin system. In the rotating frame, the angle φ_J between the two vectors in the xy plane associated with a single spin is $\varphi_J = 4\pi J_{AX} 2\tau_2$, where J_{AX} is the coupling constant (Hz) between the two spins. If our delay $2\tau_2$ is equal to $1/(2J_{AX})$ [or multiples of $1/(2J_{AX})$], then the doublets of the two nuclei will be negative in the spectrum. At values less than $1/(2J_{AX})$, additional phase components will appear in the doublet resonances. In order to avoid these there is a practical limit for the time the spins spend in the xy plane. These problems are alleviated with the stimulated echo construct shown in Fig. 2(c). The pulsed gradient stimulated echo pulse sequence essentially replaces the 180° pulse with two 90° pulses and

minimizes the time the magnetization spends in the xy plane. After the second 90° pulse the magnetization is placed back into the z direction where the relaxation is governed by T_1 . This is generally more favorable because the ratio T_1/T_2 is commonly greater than unity for ^1H nuclei. The J -modulation effects are also minimized. The signal intensity for the stimulated echo pulse sequence [Fig. 2(c)] is given as (11)

$$E_{(t=2\tau_2+\tau_1)} = \frac{1}{2} E_{(t=0)} \exp[-D\gamma^2 g^2 \delta^2 (\Delta - \delta/3) - R] \quad [7]$$

where $R = 2\tau_2/T_2 + \tau_1/T_1$. The main drawback of the sequence is that half of the total potential signal is lost. This is due to the fact that the second 90° pulse returns only the y component of the magnetization (M_y) or the x component of the magnetization (M_x) to the $\pm z$ axis, instead of both at once. The other component is either destroyed by a gradient homospoil pulse [not shown in Fig. 2(c)] or may be cancelled by an appropriate phase cycling scheme. Therefore, only half of the signal is ultimately refocused. The simplest phase cycling scheme will coadd four vectors; M_x and M_y are each placed in both the $+z$ and $-z$ axis during τ_1 . Because it is common that the T_1/T_2 ratio is greater than unity, in most cases the benefits of the stimulated echo construct generally outweigh the signal disadvantage. All of the experiments shown in this report make use of the pulsed gradient stimulated echo pulse sequence. To clarify, the acronym PGSE was used in a general sense in the literature to define the experimental approach to use an echo scheme with pulsed (time-dependent) gradients to measure diffusion, not to distinguish between the spin echo version and the stimulated echo version. Rather than trying to make a specific distinction between the two experiments, pulsed gradient stimulated echo and PGSE, the general technique is referred to as PGSE NMR.

EXPERIMENTAL

The ^1H -NMR measurements were obtained on a Varian Inova 400-MHz spectrometer equipped with a 20-A Highland gradient amplifier and a standard 5-mm indirect detection, pulsed field gradient (PFG) probe. The combination provides a z gradient strength (g) of up to 0.33 T m^{-1} (33 G cm^{-1}). Typically, a value of 200–400 ms is used for Δ , 5–10 ms is used for δ , and g is varied from 0.03 to 0.33 T m^{-1} in 12–20 steps. The g is typically varied in such a way that there are equal steps in g^2 . In fact, this procedure

is necessary for the DECRA analysis (explained further in the Data Analysis section). The values of Δ and t in Eq. [2] are chosen to be large enough so that the RMS displacement is much larger than the size of the slowest diffusion species. The combination of g , Δ , and δ were chosen to generally obtain 90–95% total signal attenuation throughout the experiment. Other parameters include the following with typical values: a sweep width of 3600 Hz, 32768 points for Fourier transform, 64 transients, and an acquisition time plus a delay of 4.5 s. Deuterium locking was used.

All data analysis was performed using Varian VNMR, Version 6.1C. The DOSY processing program as implemented in VNMR was used. The program FIDDLE, developed by Morris et al. (43), is used for reference deconvolution. DECRA processing by Windig and Antalek (18, 19) is included in the user library of the aforementioned version.

Two solution mixtures are examined in this work. The first is a mixture of 20 mg/mL glucose (α -D-glucose) and 20 mg/mL sucrose in D_2O with 3-(trimethylsilyl) propionic-2,2,3,3- d_4 acid sodium salt (TSP) as a reference at 0 ppm. It is noted that glucose will undergo mutarotation in water and over a period of hours form two anomers, which are α -D-glucopyranose and β -D-glucopyranose (44). The α and β forms exist in a molar ratio of approximately 1:2 and have anomeric protons whose resonant frequencies are 5.24 and 4.66 ppm, respectively. The anomeric proton resonance for the sucrose is 5.42 ppm. The solution was allowed to equilibrate at room temperature for 24 h prior to measurement. The second mixture is 10 mg/mL toluene, 12 mg/mL diphenylamine, and 13 mg/mL tri- p -tolylphosphine in CD_2Cl_2 with tetramethylsilane (TMS) as a reference at 0 ppm. Experiments were performed at 22°C , just slightly above room temperature. All chemicals with the exception of sucrose were obtained from Aldrich Chemical Company (Milwaukee, WI). Food grade sucrose was used.

A series of aqueous polymer solutions was examined with PGSE NMR and the results were compared with dynamic light scattering (DLS) to illustrate the utility of standard PFG equipment for measuring displacement of high molecular weight species. Aqueous (90% $\text{H}_2\text{O}/10\% \text{D}_2\text{O}$) solutions of 0.15% (w/w) poly(styrene sulfonate) sodium salt (PSSNa; molecular weight $\approx 311, 88, \text{ and } 350 \text{ kDa}$; Scientific Polymer Products, Ontario, NY) were prepared with 0.1 N sodium acetate and a pH of 7.0. The same solutions were used for both DLS and PGSE NMR.

For some of the tests described in this article a doped water (10% D₂O in H₂O + 0.1% GdCl₃) sample (Varian, Inc., Palo Alto, CA) was used.

DATA QUALITY

In order to achieve the most reliable analysis, regardless of the analytical technique, we must reduce or eliminate any experimental artifacts. The PGSE NMR experiment is susceptible to several artifacts, all of which are manageable with proper care and consideration. Before presenting the details of the artifacts, we must first identify the constituents of a good data set.

There are five elements of a good data set:

1. excellent registration of resonances,
2. no gradient-dependent spectral phase distortion or broadening.
3. good differentiation in decay among components,
4. no baseline artifacts, and
5. pure exponential decay.

These are illustrated in the data in Fig. 3. The anomeric region of the spectrum from a sample containing sucrose and glucose is shown. Because glucose is the smaller molecule, all of the resonances associated with glucose will decay with a faster rate in the data set with respect to sucrose. This is difficult to observe in a simple stacked plot of eight representative spectra [Fig. 3(a)]. It can be readily observed if we normalize each spectrum to a resonance from the slowest moving molecule [i.e., the largest in size; Fig. 3(b)]. The sucrose resonance in each of the spectra overlays each other perfectly in the normalized plot of Fig. 3(b). The glucose resonance decays about 75% more relative to the sucrose.

Every mixture analysis problem using PGSE NMR involves differentiation of the resonances based upon their diffusion coefficient. This involves the analysis of the decay rate of the resonances within the frequency domain data set. There are several ways to accomplish this differentiation and all of them assume that each peak in every spectrum is exactly the same shape but only reduced in total area and that each peak in every spectrum has the same frequency value throughout the data set. The problems in data analysis arise when this is not true. For example, if the gradient is perturbing the FID collection process, there may be a gradient-dependent systematic error, such as a phase distortion or line broadening. This anomaly is embodied in the resonances in such a way that a resonance in

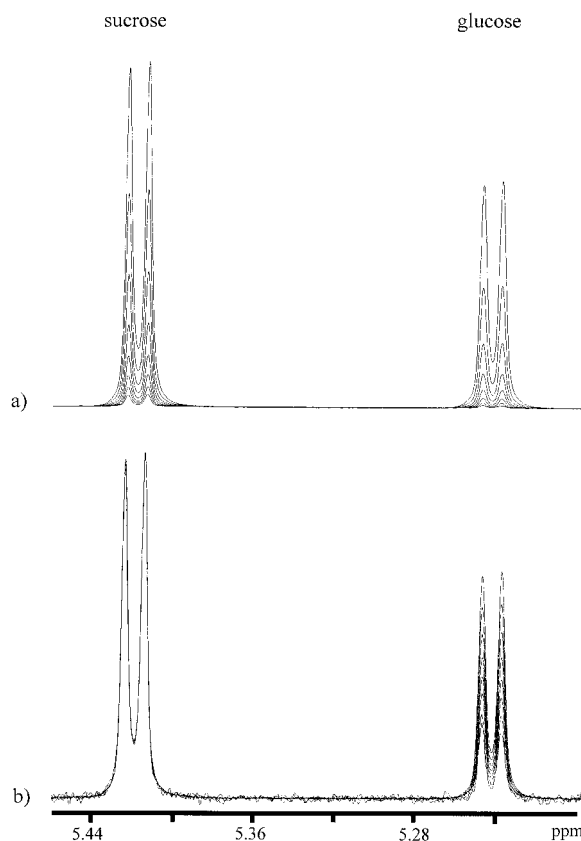


Figure 3 (a) A stacked plot of the anomeric region from eight spectra obtained from a PGSE NMR experiment performed on a mixture of glucose and sucrose. The doublet from glucose is at 5.24 ppm and that of the sucrose is 5.42 ppm. (b) The same data as in (a) but normalized to the sucrose resonance. It can be seen that the intensity of the glucose resonance decays more rapidly with respect to that of the larger, and therefore slower moving, sucrose.

the first spectrum has a different shape or spectral position than the same resonance in a subsequent spectrum. Very slight systematic errors in the spectra will cause substantial errors in the diffusion analysis and limits the ability to differentiate components based upon the molecular size. This point is illustrated in Fig. 4 where the sucrose anomeric doublet in the PGSE NMR data set is scrutinized. Ten spectra were acquired, and an average diffusion coefficient was calculated from the integrals of the resonances. A diffusion coefficient was then calculated for each frequency point in the data set. These were then subtracted from the average diffusion coefficient to obtain a measure of accuracy. Figure 4(a,b) shows the stacked plot and difference results from a high-quality data set (the same as that shown in Fig. 3). As can be seen in Fig. 4(b), the diffusion coefficients calculated from the frequency positions compare well with the

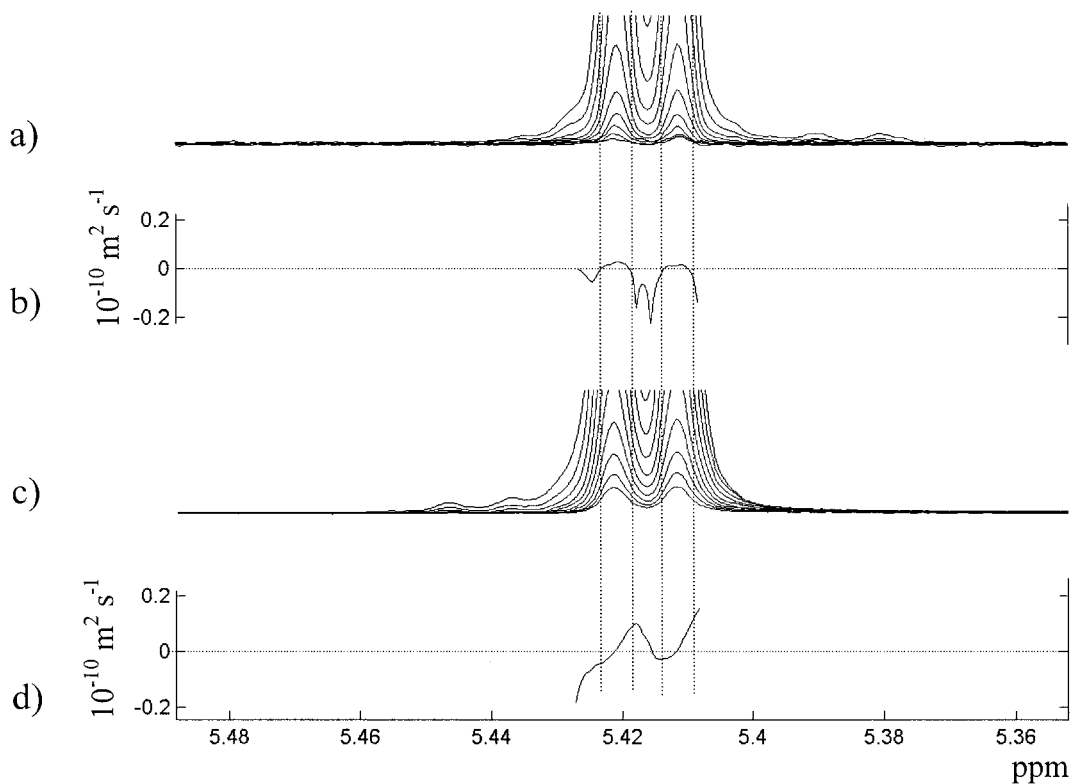


Figure 4 The effect of a minor phase distortion on the measurement of the peak signal decay in a PGSE NMR experiment. (a) A stacked plot of a high-quality PGSE NMR data set showing the sucrose anomeric doublet. No phase distortion is present and good registration is evident. (b) The plot of the difference between the average diffusion coefficient calculated from the peak integrals and the diffusion coefficient calculated at each frequency value. Note that there is very little variation directly under the two main resonances of the doublet. Only in the flanks and between the doublets are there deviations. (c) A stacked plot of lesser quality PGSE NMR data. Although the registration appears good, there is evidence of phase distortion (i.e., the lines on the right of the stack are closer together than those on the left). (d) A plot similar to the latter showing a systematic change in the measured decay exponentials directly under the two main resonances.

average, especially under the main portion of the two resonances (i.e., it is flat between the two sets of vertical dotted lines). Figure 4(c,d) shows the stacked plot and difference results from a lesser quality data set, one that contains very slight phase distortion. The phase distortion is evident in Fig. 4(c) by close inspection of the flanks. The lines are closer together on the upfield side of the doublet and more spread out on the downfield side. This results in a systematic change in the calculated diffusion coefficient for the same spectral regions (i.e., there is a significant slope in the difference data between the two sets of vertical dotted lines). Despite the fact that the spectral distortion is difficult to perceive in the data, there is nonetheless significant error in the diffusion measurement.

Other problems may exist including poor registration of the resonances in the data set, baseline drift, systematic line broadening, and so forth; these will all

affect the measured diffusion coefficient or the ability to differentiate components within a mixture in a detrimental way. Often, many of these problems are present in a single data set.

DATA ACQUISITION

Proper control of data acquisition is essential for obtaining optimum data quality. In the previous section we outlined the general attributes of a high-quality data set and how very slight, systematic deviations from the ideal case can affect the final data analysis. This section delineates the major causes of systematic anomalies in the PGSE NMR data set and how to remedy them. It is assumed that the equipment is sound. The two gradient pulses used in the experiment need to be identical, and because of this a stable

gradient amplifier is important. The gradient driver should be stable enough to deliver reproducible gradients to within 1 part in 10^5 in order to measure diffusion as slow as $10^{-13} \text{ m}^2 \text{ s}^{-1}$ (6). This can be understood by the following. Using Eq. [2], the RMS distance for a molecule having a diffusion coefficient of $10^{-13} \text{ m}^2 \text{ s}^{-1}$ measured during 100 ms is on the order of 0.1 μm . Typically, for common probes, the length of sample that is excited by the RF pulse is on the order of 10,000 μm . The encoding gradient should “twist” the xy magnetization 10^5 times (10,000 $\mu\text{m}/0.1 \mu\text{m}$). Therefore, for accurate refocusing within a few degrees the gradient area should be matched by better than 1 part in 10^5 . Additionally, the gradient should be a shielded design that allows for fast switching, at least on the order of microseconds (9).

There are essentially three problems that give rise to artifacts in the acquired spectra:

1. electrical eddy currents caused by the fast switching of the applied gradient pulse (even with actively shielded coils),
2. gradient field nonuniformity that is the result of the coil design, and
3. convection currents caused by temperature gradients.

Under most circumstances, these problems may be well controlled and the deleterious effects minimized. These are discussed in the following segments. Several pulse sequence elements are mentioned that may alleviate some of the problems, and these are summarized in a separate segment. Other issues relating to signal behavior are worth mentioning in brief and are included. Finally, the topic of calibration is included at the end of the section.

Eddy Currents

Eddy currents are electrical currents caused by the fast switching (on and off) of the gradient pulse. Whenever a magnetic field changes, eddy currents simultaneously form within any closely located conductor. These currents are set up in a way to oppose the change. The effect produces a magnetic field that can be experienced by the sample and therefore causes distortion in the spectra. Moreover, the extent of the distortion is dependent upon the strength of the applied gradient pulse and thus will produce a systematic change in the PGSE NMR spectral series. The characteristics of these eddy currents are rather involved, but the decay is generally governed by a sum of fast and slow exponentials (45). To avoid this

problem probe manufacturers designed a shielded gradient system. A secondary series of gradient coils outside the primary Maxwell pair is designed and constructed to produce a magnetic field at the inside wall of the probe body that is equal and opposite to the one formed by the primary coil. These two fields cancel and the eddy currents that would normally form in the probe body are minimized. No design is perfect and eddy currents, although greatly reduced, are still present.

In addition to directly affecting the spectral quality, eddy currents can also have an effect on the locking mechanism. The lock circuitry is designed to compensate for small changes in the main magnetic field. Depending upon the time constants built into the circuitry, it may have a response to the applied gradient pulse and even produce shifts in the resonances.

To measure the time that is required for the eddy currents to fully decay one simply applies the gradient pulse, waits a period of time, and then acquires the spectrum from a single pulse experiment. The experiment is shown in Fig. 5(a), and the result of this experiment is shown in Fig. 5(b) for a doped water sample. Each spectrum in Fig. 5(b) is acquired with a different delay time d . The results vary widely, depending on the particular probe used. In this example the full signal strength appears to recover by 200 μs . However, upon closer inspection the gradient effects still persist beyond 1 ms. Figure 6 illustrates this longer term eddy current effect. An expansion of Fig. 5(a) is shown in Fig. 6(a) with three delay times indicated. For each of these delay times the gradient strength was varied from 0 to 0.308 T cm^{-1} in 0.0193 T m^{-1} steps, and the resultant spectra are plotted in Fig. 6(b–d). All of the spectra were phased using the last spectrum in the series. Gradient-dependent phase distortion is evident for $d = 300 \mu\text{s}$ and 1 ms. None is observed for the $d = 2$ ms. This corresponds to the first spectrum in Fig. 6(a) that has the same phase as the last spectrum ($d = 1$ s).

It is evident from the previous discussion that in order to avoid gradient-dependent artifacts in the PGSE NMR data set, one must wait a period of time >1 and ≤ 2 ms after the application of the final gradient in the pulse sequence and before the data acquisition. This optimal time is also probe dependent. One could, of course, take finer steps to better determine the optimum value.

Many articles have been published that discuss ways to minimize this ring down time (45–50). All deal with either changing the shape of the applied gradient pulse (by changing the current pulse shape

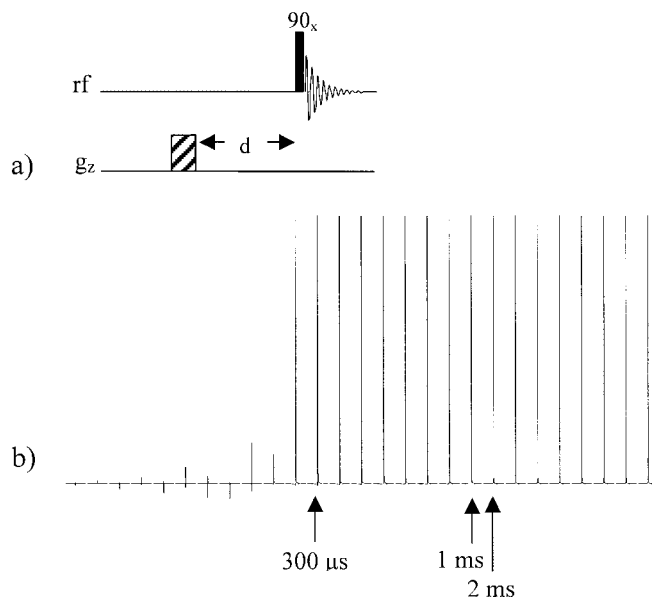


Figure 5 (a) The simple pulse sequences used to measure the effect of eddy currents on the acquired signal caused by the application of a gradient pulse. The delay (d) is varied several orders of magnitude from 10s of microseconds to 100s of milliseconds. (b) The result of a gradient recovery experiment including 27 spectra with the following d values: 10, 20, 30, 40, 50, 60, 70, 80, 90, 100, 200, 300, 400, 500, 600, 700, 800, 900, and 1000 μs ; 2, 5, 10, 20, 50, 100, 500, and 1000 ms. The gradient is a composite of two gradient pulses of 5-ms length, 0.30 T m^{-1} strength, 2 ms apart, and oriented in a bipolar fashion. No line broadening is used. For this example the major impact of the eddy currents is diminished by $200 \mu\text{s}$. The result is dependent upon the probe design, as well as the shape of the gradient pulse or the use of composite gradient pulses.

delivered to the probe) or using a gradient/RF pulse composite. Pre-emphasis has been traditionally used in magnetic resonance imaging (MRI) to help control the effects of the large gradient coils used to produce the spatially labeling fields (45). The current pulse is overdriven at the beginning and underdriven at the end using a multiexponential waveform. Because it is difficult and/or time consuming to optimize the pre-emphasis waveform, pulse shaping is an alternative, especially for lower gradient strength pulses. Typical examples are shown in Fig. 7. The advantage to changing the shape is that a gentler rise and fall will lessen the intensity of the eddy currents. The disadvantage is that they incorporate less gradient during the same time when compared with a square pulse and so will be less effective (i.e., the total area, strength \times time, of the shaped gradient is less than that of the square gradient). In fact an expression different from Eq. [6] is derived for each unique gradient shape (46). Either the ramped (or trapezoidal) pulse or the half-sine pulse [Fig. 7(a,b)] will greatly reduce the recovery time. However, they do not adequately eliminate all of the (more subtle) effects of eddy currents.

A better alternative for high resolution work is the composite. Placing two gradient pulses in opposite

polarity with a 180° RF pulse between them creates a self-compensated composite. In general, the disturbance created by the second gradient pulse in the pair offsets that of the first gradient. The 180° RF pulse is present so that the magnetization continues to dephase in the same direction during both gradients. Figure 7(c) shows the simple bipolar gradient composite, which was described for use in the PGSE NMR experiment (48). Another composite is the “CLUB sandwich” [Fig. 7(d)] (49). This composite features a high power, constant amplitude, frequency modulated inversion pulse that lies between a bipolar pulse pair arranged in a double format. The composite was originally developed as an ideal PFG pulse in an HSQC pulse sequence that provides both better suppression of unwanted magnetization and much reduced phase distortion; the shape of the inversion pulse is given by Mandelshtam et al. (50). However, a standard, hard 180° RF pulse works satisfactorily for the PGSE NMR application. Chemical shift and heteronuclear J coupling are refocused with the CLUB sandwich. Both composites were shown to reduce the lock disturbances, as well as reduce the ringdown time without losing the gradient effectiveness.

Gradient Field Nonuniformity

The basic derivation of the signal decay function described in Eq. [6] only assumes that the gradient is uniform in the z direction across the entire sample region. Deviations from a uniform gradient will cause systematic deviations from the ideal decay behavior. Once again, this effect is probe dependent and may vary widely. The problem is illustrated in Fig. 8(a) using the doped water sample at 23°C. The signal attenuation is recorded and a nonlinear least-squares fit is applied to the integrated signal of the water resonance. The residuals (i.e., the point from the fitted curve subtracted from each data point) are plotted below the data. Although at first glance the data appear to fit well on the line, a close inspection of the residuals reveals a systematic error in the data. This is caused by the fact that some signal from the sample is acquired from outside the uniform portion of the

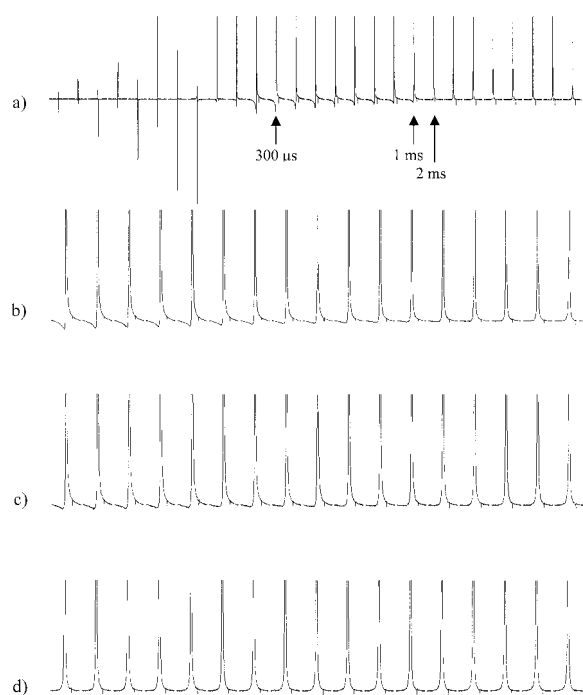


Figure 6 (a) An expansion of the spectra shown in Fig. 5(b) showing the persistence of phase distortion through 2 ms. (b) Spectra acquired with a composite gradient pulse as described in Fig. 5(b) but with a strength varied linearly from 0 to 0.308 T m^{-1} in steps of 0.0193 T m^{-1} . The delay (d) between the composite gradient pulse and acquisition is $300 \mu\text{s}$. All of the spectra are phased using the optimum values from the final spectrum. A gradient-dependent phase distortion is evident. (c) The same as the latter but with $d = 1 \text{ ms}$. A gradient-dependent phase distortion is evident. (d) The same as (b) but with $d = 2 \text{ ms}$. No gradient dependent phase distortion is evident.

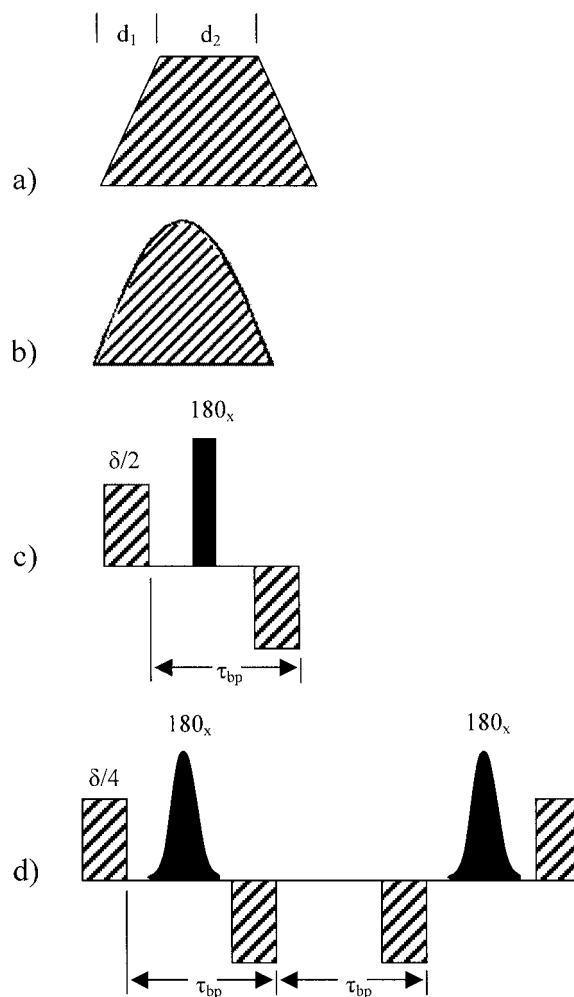


Figure 7 Alternatives to the standard square gradient. (a) The ramped (or trapezoidal) gradient shape, (b) the half-sine shaped gradient, (c) the bipolar gradient composite, and (d) the CLUB-sandwich gradient composite including two shaped 180° pulses.

magnetic field gradient. Most gradient coil designs have a “sweet spot” in the very middle of the coil that provides the most uniform gradient. This gradient strength may vary substantially (depending on the specific design) as a function of the distance from the center. Therefore, only a small portion of the sample actually experiences a strong, uniform gradient. Concurrently, most RF coil designs generally excite a region beyond the coil’s physical dimensions. This combination produces nonideal signal decay behavior (51). The probe used in the work presented here produces a stronger gradient in the middle region and a weaker gradient further from the center. Within a PGSE NMR diffusion experiment the signal from the center of the sample region decays faster than the signal from the two ends of the sample region, so the

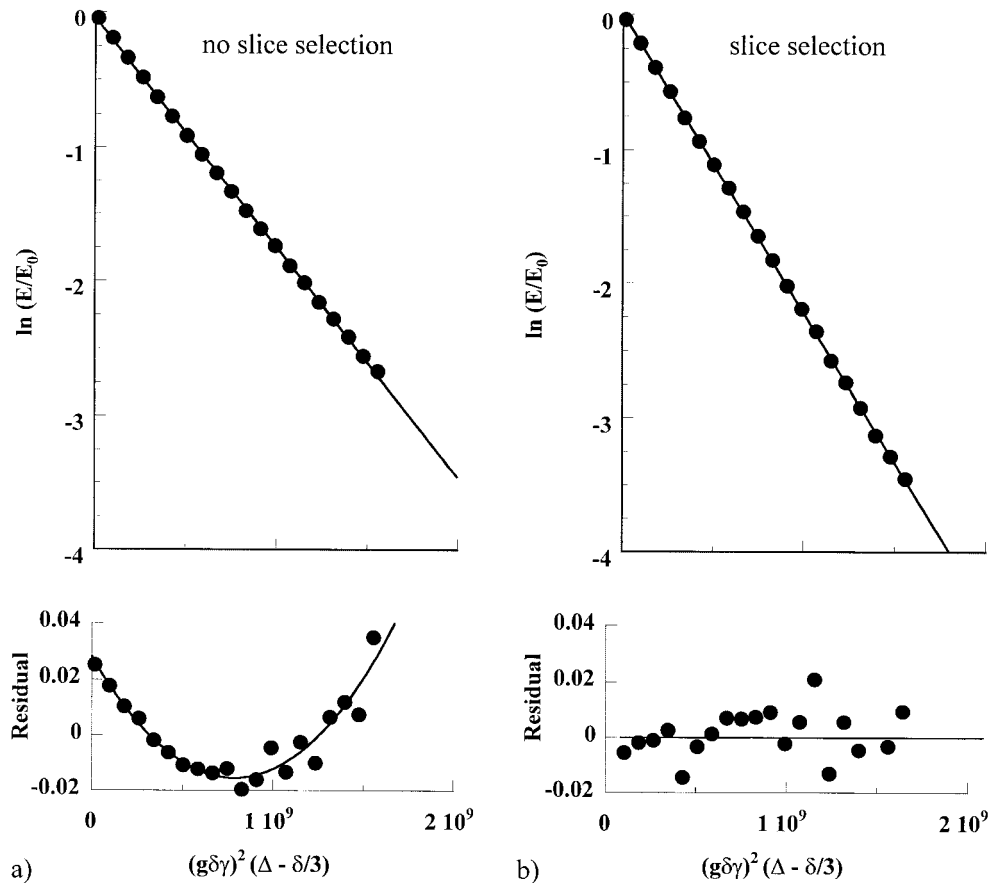


Figure 8 Signal attenuation plots from a PGSE NMR diffusion experiment of a doped water sample using the pulsed gradient stimulated echo experiment with the following parameters: $\delta = 0.0011$ s; $\Delta = 0.2$ s; and g^2 is varied linearly for 20 values from $(0.03)^2$ to $(0.33)^2$ (T m^{-1})². The line through the data is a nonlinear least-squares fit to a single exponential function. The residual, plotted below using the same abscissa, is calculated by subtracting a point on the fitted curve from the corresponding data point. (a) No slice selection is used. The line through the residuals is a simple nonlinear least-squares fit of a quadratic function to show that the deviation is systematic. (b) A slice selection step is used. The line through the residuals is a simple nonlinear least-squares fit of a linear function.

total decay has curvature. This curvature introduces considerable error with the measurement of the diffusion coefficient. For example, in Fig. 8(a) the diffusion coefficient measured from the first five points only, all of the points, and the last five points only are $(1.79, 1.71, \text{ and } 1.60) \times 10^{-9} \text{ m}^2 \text{ s}^{-1}$, respectively. The error gets worse as the extent of attenuation increases.

One way to visualize the gradient field nonuniformity is to combine the PGSE NMR diffusion experiment with the 1-D imaging profile experiment. If a gradient is turned on during the acquisition, the signal obtains a position-dependent frequency according to Eq. [4]. The signal from the top of the sample region will be on the right side of the spectrum and the signal from the bottom on the left side or vice versa, de-

pending on the polarity of the gradient. Hence, a profile of the sample region is obtained. Because the signal attenuation in a PGSE NMR diffusion experiment is dependent upon the gradient strength, one can use it in concert with the 1-D imaging profile experiment to interrogate the position-dependent gradient. Figure 9 shows the result of such an experiment using the pulse sequence elements illustrated in Fig. 10. The 1-D profile was acquired using the doped water sample and the pulse sequence shown in Fig. 10(a) with $g = 0$. The half-echo was acquired and standard Fourier transformation was used. The diffusion encoding gradient strength g was then varied and the diffusion coefficient was calculated using Eq. [6] point by point along the profile. Because the diffusion coefficient does not change in the sample, an apparent

diffusion coefficient (D_{app}) is measured. It is therefore proper to go one step further and express this variance directly in terms of g . As g^2 increases, D_{app} will increase as well. The ratio D/g^2 should be a constant (i.e., the slope is constant in the plot of $\ln E/E_0$ versus g^2 for Eq. [6]). The value of g is then calculated from

$$[(g_{\text{known}})^2 D_{\text{app}} / D_{\text{known}}]^{1/2}$$

where g_{known} and D_{known} are the known values for g at the center of the coil and the diffusion coefficient of water within the doped sample (at 23°C), which are 0.33 T m^{-1} and $2.23 \times 10^{-9} \text{ m}^2 \text{ s}^{-1}$, respectively. Across a 15-mm sample region, the gradient strength varies by about 30%. This corresponds to a variation of about 50% in the diffusion coefficient along the same dimension. Clearly, to obtain the most accurate diffusion coefficients, one has to find a way to obtain

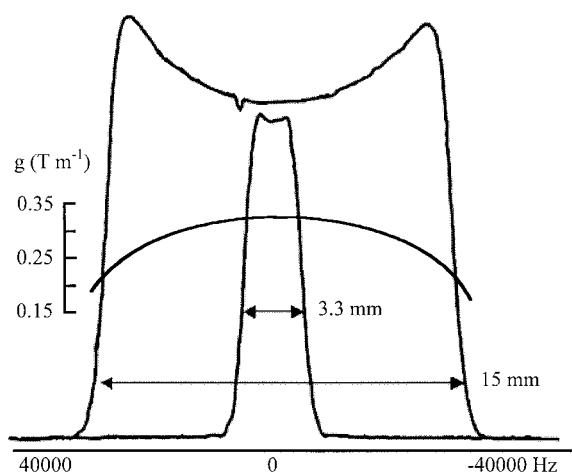


Figure 9 The 1-D profile experiment showing the effect of slice selection. The profile represents the signal obtained from an approximate 15-mm sample height, the active volume of excitation. Depending upon the polarity of the applied gradient voltage, the right side of the profile represents the top of the active volume in the NMR tube and the left represents the bottom. The smooth, concave line indicates the point by point gradient strength calculated (using Matlab 5.3, The Mathworks Inc.) from a PGSE NMR diffusion experiment with a gradient turned on during acquisition. For the probe used there is a 30% decrease in gradient strength near the top and bottom ends of the full region of the RF excitation, which corresponds to a 50% decrease in the measured diffusion coefficient. The slice selection step enables one to excite a nearly uniform region of the gradient at the expense of the signal. The typical region used is 3.3 mm. Therefore, approximately 80% of the total signal is lost. Because the gradient strength varies along the length of the tube, the distances shown are only approximate.

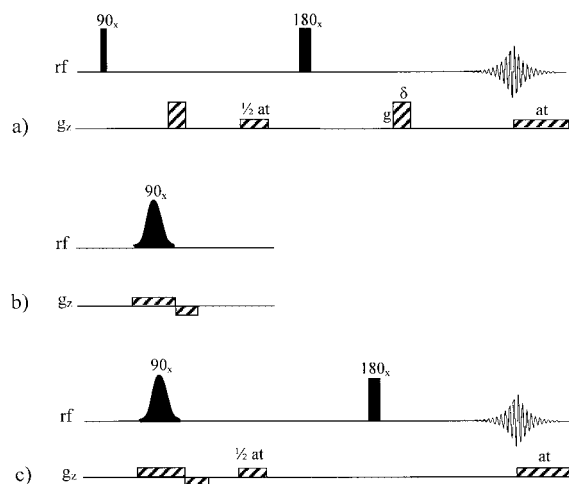


Figure 10 (a) The PGSE pulse sequence incorporating the necessary elements to obtain a 1-D image (profile) of the doped D_2O sample. A gradient is turned on during acquisition to obtain a position-dependent frequency plot. The acquisition time (at) is typically 2.5 ms and the gradient strength of the acquisition gradient is about 0.04 T m^{-1} . The gradient between the 90° and 180° pulses, indicated as $\frac{1}{2} \text{ at}$, is to correct for an added phase component produced by the gradient during acquisition. (b) The slice selection element. A shaped pulse is applied while a gradient is turned on in order to select a narrow frequency band, and hence a narrow section in the middle of the sample region. (c) The pulse sequence incorporating both the slice selection and profile elements (but not the diffusion gradients).

a signal from only a small region in the center of the sample.

There are two approaches that may be used to obtain a signal from within only the uniform region of the gradient: physically constrain the sample to that region or excite only the spins in that region. The former requires the use of properly matched susceptibility tubes or inserts. Depending on the style, it will not allow one to completely get away from placing the sample beyond the uniform region. Some styles are designed to incorporate a film of solvent between the plug and tube wall. The better approach involves a step called slice selection that is used in MRI. The idea is to use the gradient in concert with a selective RF pulse to excite only those spins in the middle of the sample region. Figure 10(b) shows the slice selection element. We simply choose an excitation pulse shape with a calibrated excitation bandwidth and, using Eq. [4], match the bandwidth with the gradient strength in order to excite the uniform region. In this example, for the slice selection element we use a Hermitian-90 pulse shape (52) with an excitation bandwidth of about 8 kHz and a slice selection gradient of 0.043 T m^{-1} strength to achieve a slice

thickness of approximately 3.3 mm. The pulse sequence in Fig. 10(c) was used to produce the narrow profile shown in Fig. 9. The gradient strength used in the acquisition step to obtain the 1-D profiles in Fig. 9 is arbitrary; 0.13 T m^{-1} was used. One should ultimately choose an excitation bandwidth greater than the spectral bandwidth in order to equally excite all resonances. The compromise with this approach, of course, is signal to noise (S/N). In the example given above, 80% of the signal is lost.

The result of slice selection is realized in Fig. 8(b). The same experimental parameters and processing steps as in Fig. 8(a) were used. The residuals from the decay are random and center about the zero position. No systematic change is apparent, although the noise level is actually larger. Analyzing the diffusion coefficient measured from the first five points only, all of the points, and the last five points only that are obtained, which are $(2.25, 2.23, \text{ and } 2.22) \times 10^{-9} \text{ m}^2 \text{ s}^{-1}$, respectively. These values are within 1% of each other. They are also higher in magnitude because the gradient strength is higher in the middle of the sample region. For the probe used here the average overall increase in gradient strength is 13%. The slice selection pulse should be as short as possible to minimize phase shift problems, and the slice thickness should be as large as possible so that diffusion in and out of the active region does not significantly contribute to the final signal decay.

Temperature Gradients

Arguably, the most difficult problem to control is temperature gradients. Most modern NMR systems introduce variable temperature (VT) air through the bottom of the sample region. The VT gas then travels around the side of the tube and exits through a port near the top of the sample region. There is very little room to spare. Because the probe is generally optimized for maximum S/N, the RF coil is as close as possible to the sample tube. This can easily create a situation where the bottom of the tube experiences warmer gas than the top (or vice versa if cold gas is used to cool the sample). The fact that glass is a good insulator only exacerbates the problem. Although one can achieve an average temperature, there may still be a temperature gradient along the long axis of the tube. Depending on the viscosity of the solvent inside the tube, temperature gradients can cause convection currents to establish and persist. This adds a velocity term to the diffusion and will perturb the ideal decay in a PGSE NMR experiment by superimposing an oscillating behavior in the signal decay, and it can actually create negative signals (53, 54). The effect of

flow on the NMR signal is well understood (6, 55) and was utilized for MRI (56, 57) and electrophoretic NMR (58).

Several formal methods were presented to measure or visualize thermal convection (59–63). To simply observe the effect one needs to allow the signal in the PGSE NMR experiment at the proper temperature to attenuate at least 95% and examine the decay behavior. If there is no effect from the temperature and effects from gradient field nonuniformity are eliminated, the decay should be linear on a semilogarithmic plot. Figure 11 demonstrates the effect using the sucrose/glucose sample. Three experiments are performed at 45°C using a standard 5-mm PFG probe. All experimental and processing parameters were kept the same, except for the rate of spin and the sample tube size. Evidence of convection currents caused by temperature gradients is found in the 5-mm no spin case. As shown in Fig. 11(a), the resonances begin to exhibit phase distortion for the higher gradients. This is realized as a precipitous drop in signal intensity as shown in Fig. 11(b). If allowed to decay further, it is expected that the signal would become negative before cycling back to positive again.

Spinning a sample tube is, in principle, allowed in the PGSE NMR experiment because it introduces velocity terms orthogonal to the z direction. Two studies showed the suppression of effects from convection currents using sample spinning (64, 65). How it suppresses the convection is rather complicated, and it is described elsewhere (66). The sample in the 5-mm tube was allowed to spin at a rate of 18 Hz, and the result is shown in Fig. 11(b). Although spinning greatly alleviates the problem, there is the possibility of introducing other problems such as vibrations. An alternative is to simply use a smaller size tube, such as 3 mm (at the expense of S/N). The results are shown in Fig. 11(b). Note that the slope of the spinning data is slightly steeper than that of the 3-mm data. Although convection is greatly reduced by sample spinning, it is not completely eliminated. The effects of convection may be present before nonlinear decay behavior becomes apparent.

In addition to the sample diameter, it makes sense to reduce the sample height as low as possible without compromising the line shape. However, the effect of reducing the sample diameter is much more important than reducing the height. Therefore, reducing the height should be done only after the diameter is reduced as much as is tolerable. The VT gas flow rate should be high enough to allow for thorough heat transfer along the tube but not so high as to introduce vibrations. Depending on the probe design, 10–15 L/min should be adequate. Goux et al. describe the

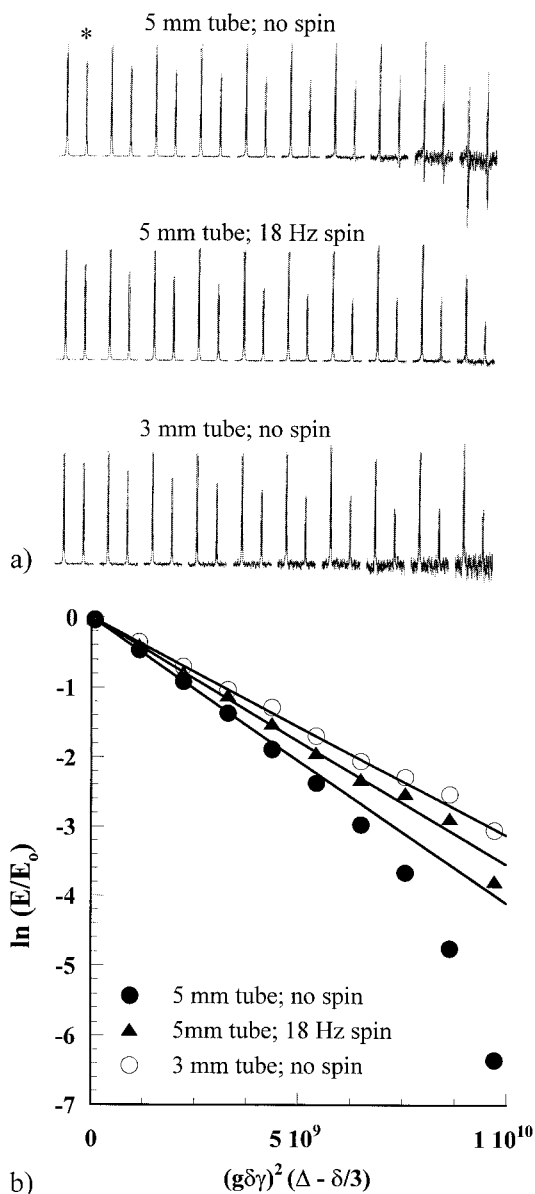


Figure 11 The effect of temperature gradients on the PGSE NMR data. (a) Normalized plots from three PGSE NMR experiments showing the anomeric proton region of the spectrum for a sample containing glucose and sucrose dissolved in D_2O . (*) The glucose anomeric proton is indicated. (b) Signal decay plots from the glucose resonance in the data shown in the former. The lines are a nonlinear least-squares fit of a linear function from the first three points only in each data set.

effects of the VT air flow rate, tube diameter, and sample height on PGSE NMR experiments (67).

Another solution is to use a convection current compensated pulse sequence (68–70). This method uses the concept of “moment nulling” (57), which relies on a double stimulated echo configuration,

where the gradient direction is reversed in the second echo sequence with respect to the flow, thereby canceling its effect. Bipolar versions were introduced and the pulse sequence was shown to perform well for both warmed and chilled samples (69, 70).

Pulse Sequence

Three general problems, eddy currents, gradient field nonuniformity, and convection currents, were discussed, along with the approaches for optimizing the PGSE NMR experiment to minimize their subsequent effects. Incorporating the necessary pulse sequence elements to alleviate these problems was previously considered in the literature (65, 71–75). Tillet et al. (72) use slice selection and the incorporation of a presaturation step for water suppression. Wu et al. (71) describe the incorporation of the bipolar gradient pulse pair, as well as a longitudinal eddy current delay (LED) period, in a sequence called bpped. Pelta et al. (73) masterfully compare and contrast six pulse sequences and describe the finer points that allow a precise measurement of diffusion on the order of 1%.

A pulse sequence that incorporates the necessary elements for optimizing the experiment is shown in two forms in Fig. 12. Figure 12(a) is a variation of the pulsed gradient stimulated echo experiment shown in Fig. 2(c), and it is closely modeled after the sequence gcstesl described by Pelta et al. (73). It will be referred to as egsteSL, enhanced gradient stimulated echo with spin lock. It includes four key enhancements from the basic pulsed gradient stimulated echo experiment that enables one to obtain an optimum data set: presaturation for solvent suppression, slice selection for gradient field nonuniformity problems, bipolar gradient pulses for eddy current problems, and a spin lock step for elimination of unwanted phase anomalies. The phase cycling is listed in Table 1 and typical parameters are included in the caption of Fig. 12. Figure 12(b) is the same pulse sequence as egsteSL, but it incorporates the club-sandwich gradient composite and will be referred to as egsteSLc. It has the advantage of lowering the gradient duty cycle by a factor of 2, as well as allowing for smaller recovery delays within the sequence. It is more useful when examining larger molecular weight species that require the use of larger gradient areas and smaller τ_2 delays. A rigorous derivation of the signal decay function was not made by the author to describe the decay resulting from the egsteSLc pulse sequence, but the difference in the signal decay behavior between egsteSL and egsteSLc was undetectable using the same total gradient pulse area.

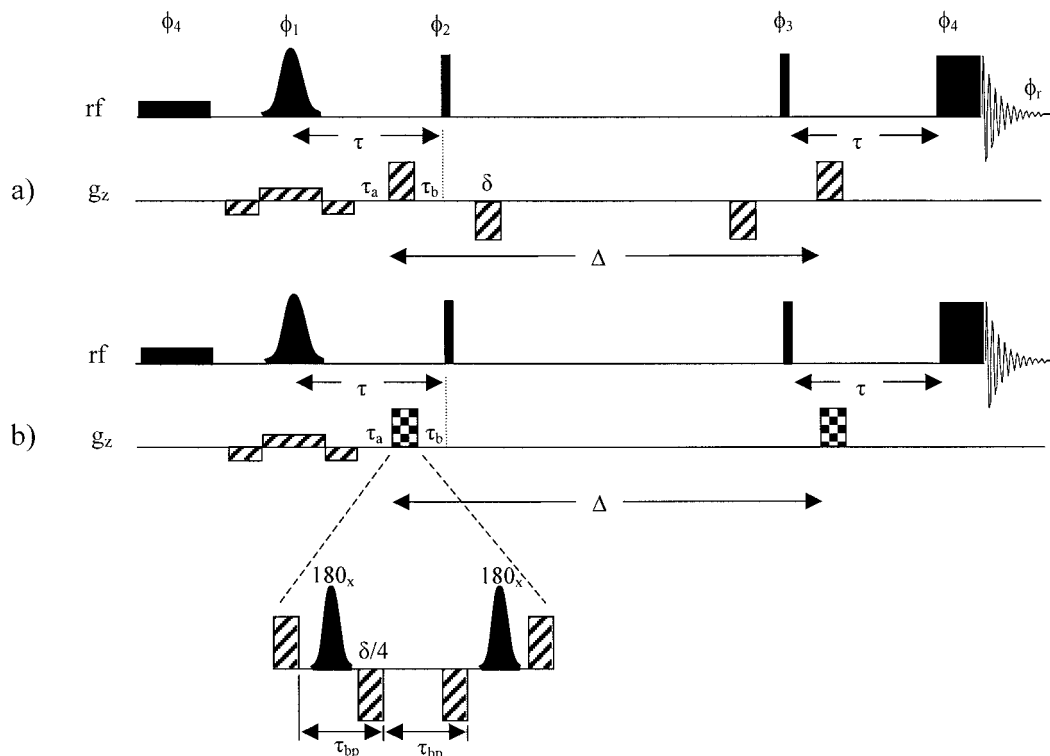


Figure 12 Pulse sequences incorporating elements necessary for minimizing the effects of gradient nonlinearity and eddy currents. (a) egsteSL, enhanced gradient stimulated echo with spin lock. Four elements are included that enable optimum data purity: presaturation, slice selection, bipolar gradients, and spin lock pulse. The presaturation is optimized as usual for single resonance suppression. The slice selection step includes a gradient composite with a typical strength of 0.043 T m^{-1} and a shaped pulse comprising a Hermitian-90 shape of $800\text{-}\mu\text{s}$ length and an 8-kHz bandwidth. The first negative gradient of the slice selection composite is half the length of the main gradient and acts in the same manner as a bipolar arrangement by minimizing lock perturbation. The second negative gradient, again half the length of the main, acts to correct for an added phase component brought about by the shaped pulse–gradient combination. The main bipolar gradients are equally spaced about their respective 90° RF pulses. The spin lock pulse is the same strength as the main 90° RF pulses but is typically 0.5 ms in length. Typical delays for τ , τ_a , and τ_b for the probe used in this study are $4\text{--}8$, 2 , and 1 ms , respectively. (b) egsteSLc, enhanced gradient stimulated echo with spin lock and incorporating the CLUB sandwich. The pulse sequence is exactly the same as in the latter except that the main diffusion gradients are replaced by the CLUB-sandwich composite. Note that the gradients between the second and third RF pulses are eliminated and thus reduce the overall gradient duty cycle by at least a factor of 2. Typical delays for τ , τ_a , τ_b , and τ_{bp} for the probe used in this study are $2\text{--}6$, 0.5 , 0.5 , and 0.5 ms , respectively. The shape of the inversion pulse in the CLUB-sandwich composite is given by Mandelshtam (50). The length is $112 \mu\text{s}$, and the power is the same as the other 180° pulses. A typical value for $\tau_{bp} - \delta/4$ is $352 \mu\text{s}$.

Other Considerations

Besides the three main concerns previously outlined, there are other minor considerations to bear in mind while obtaining PGSE NMR data. The lock should be well controlled throughout the experiment. Because the gradients temporarily perturb the field, the lock circuit should be blanked during the gradient. If possible, the time constant controlling the response of the lock to field perturbations should be lengthened in

order to accommodate the decay of the eddy currents. One should collect data in an interleaved fashion; after collecting some fraction of the total transients, for example, 16 out of 128, move on to the next gradient strength and so on. This will average any random errors that may occur and should allow for proper resonance registration.

Vibrations at the probe should be minimized. As mentioned previously, the air flow in some probes

Table 1. 64-Step Phase Cycling Scheme for egsteSL and egsteSLc Pulse Sequences

RF Step	Phase Cycling Scheme
ϕ_1	$(0\ 2\ 1\ 3)_{16}$
ϕ_2	$(0_8\ 2_8)_2\ (1_8\ 3_8)_2$
ϕ_3	$((0_4\ 2_4)_2\ (1_4\ 3_4)_2)_2$
ϕ_4	$1\ 1\ 0\ 0\ (3\ 3\ 2\ 2)_2\ 1\ 1\ 0\ 0\ (2\ 2\ 1\ 1\ (0\ 0\ 3\ 3)_2\ 2\ 2\ 1\ 1)_2\ 3\ 3\ 2\ 2\ (1\ 1\ 0\ 0)_2\ 3\ 3\ 2\ 2$
ϕ_r	$0\ 2\ 3\ 1\ (2\ 0\ 1\ 3)_2\ 0\ 2\ 3\ 1\ (1\ 3\ 0\ 2\ (3\ 1\ 2\ 0)_2\ 1\ 3\ 0\ 2)_2\ 2\ 0\ 1\ 3\ (0\ 2\ 3\ 1)_2\ 2\ 0\ 1\ 3$

Adapted from Pelta et al. (73). The numbers represent the following: 0 = 0°, 1 = 90°, 2 = 180°, 3 = 270°, and $(0_2\ 2_2)_2 = 0^\circ\ 0^\circ\ 180^\circ\ 180^\circ\ 0^\circ\ 0^\circ\ 180^\circ\ 180^\circ$.

may cause vibrations and should be optimized to prevent this. It is best to isolate the magnet from building vibrations.

Other factors that are not related to hardware but instead related to the specific chemical interactions among the solution components can affect the general analysis by disrupting the spin labeling scheme by the gradients of the PGSE NMR experiment. Such factors are cross relaxation and chemical exchange. Cross relaxation involves the exchange of magnetization between spins of different molecules. This is common between water and proteins or molecules that undergo binding. The general effect is that D will change as a function of the diffusion time (Δ) when the stimulated echo version is used (76, 77). In addition, the signal decay for the specific nuclei involved becomes nonideal (multiexponential); this was described quantitatively (76). This effect is not seen with the spin echo version. Chemical exchange can also affect the diffusion experiment (78). Not only will the decay become nonideal for the species involved, but also the signal can modulate as a function of the delay τ_2 (see Fig. 2). Furthermore, when no gradient is applied, the signal will also modulate as a function of the chemical shift. The effects of modulation may be removed with the use of the bpped pulse sequence (78) because of the action of the 180° pulse (between the bipolar gradient pair); the chemical shift evolution is refocused. However, the nonideal decay behavior will remain. Generally speaking, if the time evolution of the specific interaction (whether it be magnetization exchange or chemical exchange) is very fast or very slow with respect to the two delays (τ_1 and τ_2), the effects are not seen. If the evolution is similar to the timing delays, on the other hand, the effects will influence the analysis.

Calibration

Every gradient probe will have its own characteristic gradient strength for a given current value. This strength is calibrated by relating the gradient driver control parameter, usually a digital to analog conversion (DAC) value, to the gradient strength value.

There is a simple procedure to estimate this calibration value using the 1-D profile pulse sequence in Fig. 10(a) without the diffusion gradients ($g = 0$) to obtain a profile with a known DAC value. Use Eq. [4] to estimate the gradient strength knowing the frequency width of the profile and the approximate excitation length (i.e., the length of the sample that is actually excited by the RF coil). In the case illustrated in Fig. 9, we have a frequency difference of 80 kHz, a sample length of 15 mm, and use a DAC value of 6000 out of a total of 16,384. Using Eq. [4] we estimate a gradient strength, $g = \omega/\gamma z = 80\ \text{kHz}/(4.26 \times 10^7\ \text{Hz T}^{-1} \times 0.015\ \text{m}) = 0.125\ \text{T m}^{-1}$. Knowing our maximum gradient strength to be $0.33\ \text{T m}^{-1}$, this result makes sense because $(6000/16,384)0.33 = 0.121\ \text{T m}^{-1}$. The gradient calibration constant is then $0.125/6000 = 2.08 \times 10^{-5}\ \text{T m}^{-1}\ \text{DAC}^{-1}$. It is often written in terms of current (A). Knowing that the gradient driver can deliver 10 A for a DAC value of 16,384, the gradient calibration constant can be written as $0.0341\ \text{T m}^{-1}\ \text{A}^{-1}$.

Whereas this is only an estimate, one needs to go a step further to obtain the proper gradient calibration value. The best way to obtain this value is to use a solution with a compound having a known diffusion coefficient (D_{known}). The temperature, solvent conditions, and concentration need to be controlled. Table 2 gives a list of typical calibration solutions (79–82). Using an estimated gradient calibration constant ($g_{\text{cal}_{\text{est}}}$), perform a PGSE NMR experiment on a typical calibration sample (i.e., doped water at 25°C) and measure the diffusion coefficient (D_{meas}). The actual gradient calibration constant (g_{cal}) can be calculated from the following:

$$g_{\text{cal}} = \left(\frac{g_{\text{cal}_{\text{est}}} \times D_{\text{meas}}}{D_{\text{known}}} \right)^{-1/2} \quad [8]$$

In order to test the performance of the experiment through a temperature range, one may use a number of calibration samples. Lamanna et al. (83) used the following model to describe the diffusion coefficient of water through the full liquid range:

Table 2. Calibrations Used for PGSE NMR

Standard	Temperature (°C)	D ($\times 10^{-10}$ m ² s ⁻¹)	Reference
D ₂ O (99.9%)	25	19.0	79
D ₂ O (99.9%)	45	30.3	79
90/10 H ₂ O/D ₂ O (% w/w)	25	22.7	79
<i>n</i> -Dodecane	5	5.45	80
<i>n</i> -Dodecane	25	8.11	80
<i>n</i> -Dodecane	45	11.5	80
21 kDa MW PEO ^a in D ₂ O	25	0.351	81
160 kDa MW PEO ^a in D ₂ O	25	0.0874	81
570 kDa MW PEO ^a in D ₂ O	25	0.0238	81
212 kDa MW PS ^b in CCl ₄	25	0.347	82

^a PEO, 0.05% (w/w, dilute conditions) narrow molecular weight distribution poly(ethylene oxide) standards from Tosio Bioseep Corporation (Montgomeryville, PA).

^b PS, 10% (w/v) narrow molecular weight distribution poly(styrene) from Scientific Polymer Products, Inc. (Ontario, NY).

$$D = D_0 T^{1/2} \left(\frac{T}{T_s} - 1 \right)^\alpha \quad [9]$$

Here the model describes the non-Arrhenius behavior of water diffusion where $D_0 = 0.870$, $T_s = 225$, and $\alpha = 1.66$, where D is in units of square nanometers per second and T is in Kelvin. We used Eq. [9] to characterize the diffusion coefficient for residual H₂O in D₂O and found the following parameters: $D_0 = 0.774$, $T_s = 238$, and $\alpha = 1.46$. This also consistent with Longworth (79) and Mills (84). Holz et al. (80) characterized the Arrhenius behavior of the self-diffusion coefficient of *n*-dodecane through a temperature range of 5–55°C using the model, $\ln(D) = C_1 + C_2 [1000/T]$, where C_1 and C_2 are 5.3193 and -1.6483, respectively, and D and T are in the same units as previously.

In order to test the performance of the system through a range of diffusion coefficients, it is best to examine solutions of a polymer having a narrow molecular weight (M) distribution. Poly(ethylene oxide) (PEO) is recommended and is available in very narrow weight fractions. Furthermore, all of the signal is under one resonance, which makes it possible to examine very low concentrations. Chari et al. (81) studied the scaling of PEO with M and compared the case with and without micelle (sodium dodecylsulfate) saturation. For the polymer without surfactant, the diffusion coefficient scales with M as $D \sim M^{-0.54}$ through a range of M from 1 through 1000 kDa. For 0.05% (w/w) D₂O solutions of PEO at 25°C, the expression for the diffusion coefficient was found to be $D = 841.6 M^{-0.544}$. This is consistent with the work of Waggoner et al. (85).

DATA ANALYSIS

There are several ways to process a PGSE NMR data set in order to differentiate components based upon their diffusion coefficients. No single data analysis method can provide the user with all of the attainable information, and therefore a combination of several may have to be applied. All of the methods will benefit from obtaining the best possible quality data.

The PGSE NMR data set comprises a set of Fourier transformed spectra acquired at different gradient areas. Mixture analysis based on diffusion differentiation is intended to solve the following functional form (15):

$$E(q, \nu) = \sum_n A_n(\nu) \exp[-D_n q^2 (\Delta - \delta/3)] \quad [10]$$

where $q = \gamma g \delta$, and $A_n(\nu)$ is the amplitude at a frequency value of the n th pure component in solution having a diffusion coefficient of D_n , and $A_n(\nu)$ can be thought of as the spectrum of a pure component in the mixture that is attenuated in the PGSE NMR experiment by an exponential function having a time constant controlled by D_n . Whereas Eq. [6] describes the signal attenuation for a single resonance, Eq. [10] was generalized to represent the sum of the spectra from all of the pure components in the mixture. Equation [10] does not include a term for a velocity component and the relaxation factors are included in $A_n(\nu)$. Equation [10], as written, only accounts for cases where discrete diffusion coefficients exist. That is, the translational motion of every component in the solution is characterized by one diffusion coefficient. This will be true for pure compounds allowed to experience free diffusion (i.e., not restricted) and will not be

true for polymers whose molecular size may vary substantially.

The goal of the mixture analysis is to obtain a set of pure component spectra with their respective diffusion coefficients. Depending on the analysis method, there are essentially two ways one can represent or display the data: a 2-D plot with the frequency in one dimension and the diffusion coefficient in the other, and a set of resolved pure spectra with respective diffusion coefficients. In general, methods that produce the former are termed DOSY and the latter are termed curve resolution. The choice will depend upon the exact nature of the problem. In some cases it will be important to simply use diffusion as a means to assign a portion of the spectrum. A specific DOSY method should suffice. In other cases it may be important to obtain the full spectrum of one or several of the components. Curve resolution or a combination of DOSY and curve resolution may be necessary. The following sections describe the DOSY and DECRA approaches and briefly mention others. Included are details of the strengths and weaknesses of each approach.

DOSY Methods

There are several DOSY methods reported (15). All involve the stepwise analysis of single frequency values or small groups of frequency values. The simplest approach is to model the data set as a group of pure components represented by fully resolved resonances and having discrete diffusion coefficients. One simply calculates a single diffusion coefficient (e.g., using a linear least-squares approach) for each frequency value (sometimes called data channel) above a threshold and creates the 2-D plot (29). To better display the data, a second step is applied after the calculations are made in order to group diffusion coefficients measured for a given resolved resonance; each resonance contains several data points. A statistical analysis is made on the set and a “cross peak” is created having a width in the diffusion dimension that is representative of the standard deviation found for the values calculated for the entire resonance. As can be seen from Fig. 4, very slight deviations in the data, such as a very small phase error, can significantly affect the width of the cross peak in the diffusion dimension and spoil the diffusion resolution. However, with high-quality data this method has several advantages. No *a priori* knowledge of the system is necessary. In principle, there is no limit to the number of resolved components. Great precision in the diffusion dimension may be attained; differences as little as 1% are reported (29, 73). The limitation of the method is that

the resonances have to be completely (baseline) resolved. If more than one pure component is represented under a resonance, the measured diffusion coefficient will be a weighted average of all of those components because the method delivers one diffusion coefficient per frequency value. Another limitation is the dynamic range in the diffusion dimension. Usually one can only reasonably apply the method for species within a diffusion window of 2 orders of magnitude. Otherwise a peak may only exist in a small fraction of the entire data set (i.e., the first few spectra).

Line-shape consistency and signal decay purity are very important in the analysis for obtaining excellent precision in the diffusion dimension. To obtain the most consistent line shape throughout the data set, reference deconvolution (43) can be performed prior to the diffusion analysis. This requires a reference peak that is prominent in all of the spectra. TMS or TSP are often used and because they are rather small molecules there is a limitation in the available range of the diffusion dimension. In principle, however, any well-resolved reference peak may be used. Morris et al. developed a computer program called FIDDLE that performs reference deconvolution (43). Reference deconvolution can correct for minor inconsistencies in the spectra but cannot correct for multiexponential signal decay. Damberg et al. (86) described an additional postprocessing step that corrects for non-uniform gradient fields and they showed improvement in the precision of the diffusion dimension. Again, this method assumes baseline resolution.

Johnson and Morris (15–17) pioneered more formalized DOSY analyses. These approaches focused on solving the inverse Laplace transform (ILT) to directly obtain spectral intensities of pure components in the frequency dimension along with a “spectrum” of diffusion coefficients in the diffusion dimension. Equation [10] represents each frequency value in the PGSE NMR data set in terms of a sum of discrete exponentials with q^2 as the independent variable. This equation may be generalized to incorporate continuous exponentials:

$$E(q, \nu) = \int_0^{\infty} g(D, \nu) \exp[-Dq^2(\Delta - \delta/3)] dD \quad [11]$$

where D now can be continuous and $g(D, \nu)$ represents a spectrum of diffusion coefficients (for each frequency), the sum of which provides one dimension in the 2-D DOSY plot. We note that Eq. [11] will reduce to Eq. [10] if $g(D, \nu)$ is represented as a sum of Dirac delta functions (87):

$$g(D, \nu) = \sum_n A_n(\nu) \delta_{\text{Dirac}}(D - D_n) \quad [12]$$

The δ_{Dirac} symbol is used to represent the Dirac delta function and is defined by the following two properties:

$$\delta_{\text{Dirac}}(D - D_n) = 0 \quad \text{if } D \neq D_n$$

and

$$\int \delta_{\text{Dirac}}(D - D_n) dD = 1 \quad \text{if } D = D_n$$

The Dirac delta function enables us to define $g(D, \nu)$ as discrete.

In Eq. [11] the $E(q, \nu)$ is the Laplace transform of $g(D, \nu)$. It is the task of the DOSY processing to invert the PGSE NMR data set with respect to q^2 so that $g(D, \nu)$ may be determined. This requires calculating the ILT of $E(q, \nu)$. This is a classic physics problem, and it is very difficult to extract useful information without *a priori* knowledge to limit the possible solutions. The difficulty stems from the problem of resolving components of a multiexponential decay (87). Within experimental error or under the condition of noise, several solutions may be found that will satisfactorily reproduce the original data. Morris and Johnson (17) successfully used programs by Provencher and colleagues (88–90) to perform the data inversion with the application of constraints. Two methods, DISCRETE (88) and SPLMOD (89), treat the data set as containing discrete diffusion coefficients. Another method, CONTIN (90), treats the data set as having continuous distributions of diffusion coefficients. The latter is applicable for polymers because they have a distribution in their molecular weight (and hence a distribution in size). Another method described by Delsuc and Malliavin (91) uses maximum entropy methods to perform the ILT. Although some differences between methods involving Provencher's programs and those that involve maximum entropy exist, they provide similar outcomes.

The advantage of these methods is that they can be applied to a wide variety of chemical mixtures including polymers, giving not only the average diffusion coefficient, but also the distributions. In principle, there is no limit to the number of components that may be included in the analysis if all of the resonances are well resolved. The main limitation, however, is in the case of spectral overlap. Two criteria will limit the outcome of the analysis: the number of components and the differences in the magnitude of the diffusion

coefficients. The practical limit in spectral overlap is about three to four components and the difference in their diffusion coefficients generally needs to be at least a factor of 2 (16, 87). Typically, DOSY analysis requires very high S/N (i.e., >1000) and many spectra (i.e., >15).

DECRA Approach

Other approaches involve the resolution of components from a complete bandshape analysis. DECRA is one such curve resolution technique. For these methods, a 2-D plot is not generated; but simply a stacked plot (or individual plots) of the resolved pure components is generated, along with a list of the corresponding diffusion coefficients. The attributes that make it unique from DOSY will be discussed.

The PGSE NMR data set may be thought to have the following structure:

$$\mathbf{D} = \mathbf{C}\mathbf{P}^T \quad [13]$$

where \mathbf{D} is a matrix of n spectra containing m data points each (size nm ; n rows and m columns), \mathbf{C} is the matrix of size nr containing concentration profiles for each of the r pure components, \mathbf{P} is the matrix of size mr containing the spectra for each of the r pure components, and T stands for the matrix transpose. This is a classic problem in spectroscopy. Data representing mixtures are the superposition of the spectra of the individual (pure) components weighted by their composition. The solution is trivial if the pure spectra are known. However, if not known the solution is not simple at all. As such, there is a great body of work devoted expressly to solving Eq. [13] for \mathbf{C} and \mathbf{P} (92). The problem lies in the fact that there are an infinite number of solutions possible. Many methods involve the use of constraints such as pure variables, nonnegativity, and so forth. A pure variable is a point in the spectrum (wavenumber, ppm value, etc.) that changes within the data set due only to a single pure component. This often does not hold true and even so, the results may vary widely.

Kubista and Scarminio (93, 94) showed that it is possible to obtain only one solution (the correct solution) to Eq. [13] if two data sets exist that are proportional, as is shown with Eqs. [14] and [15].

$$\mathbf{A} = \mathbf{C}\mathbf{P}^T \quad [14]$$

$$\mathbf{B} = \mathbf{C}\beta\mathbf{P}^T \quad [15]$$

The diagonal matrix β of size rr defines a scaling factor between data sets \mathbf{A} and \mathbf{B} . Booksh and Ko-

walski (95) later showed that the Kubista method may be expressed in terms of the generalized rank annihilation method (GRAM) and that the problem can be solved analytically (i.e., no iterative or “best fit” method). For details about GRAM, see (96,97). With the two proportional data sets in hand one can then resolve the pure spectra and the diffusion coefficients without *a priori* knowledge of the spectral bandshapes of the pure components. How does one obtain the two data sets required for the analysis? Schulze and Stilbs (98) used the Kubista method on data acquired from a variation of the conventional PGSE NMR experiment that produced two correlated data sets but at the expense of the spectral bandshape. Antalek and Windig (18,19) showed that one may obtain two data sets from a single, conventional PGSE NMR data set by splitting the set into two parts; we called the method DECRA. By using data from a single PGSE NMR experiment, problems relating to spectral registration and spectral distortion are eliminated.

Typically, two data sets are constructed such that one contains spectra 1 to $(n - 1)$ and the other contains spectra 2 to n . The two data sets are proportional because of their exponential nature. This is described by Windig and Antalek (20) and is illustrated in Fig. 13. Let us start with an example data set **D**, containing four spectra from a simulated PGSE NMR experiment and shown in Fig. 13(a). Each of the four spectra in the data set is a mixture spectrum comprising two pure spectra that are weighted by a concentration factor. Because it is a PGSE NMR experiment, each pure component spectra has a concentration profile that is exponential. Therefore, the analysis assumes that the spectra from each component in the mixture decays with a pure (discrete) exponential. The first step is to split the data set into two parts, **A** and **B** [shown in Fig. 13(b,c)]. There is an infinite number of pairs of pure spectra that when combined will reproduce each of the mixture spectra. Two such solutions are shown in Fig. 13(d). The two data sets, subset **A** and subset **B**, are shown on the left. Note that the vertical scale is different for each. The two possible pairs of spectra (I and II) that may be resolved are at the top. The concentration of each of the resolved pairs within each mixture spectrum is shown in the boxes. For example, $27 \times$ (left spectrum in spectral pair I) + $8 \times$ (right spectrum in spectral pair I) = spectrum 1. Because within data sets **A** and **B** the concentration profiles for each pure component is exponential, the correct solution comprises two pure component spectra whose concentrations are proportional between the two data sets. Thus, the two data sets are proportional. For example, if we compare the concentrations of the pairs of spectra (spectrum 1

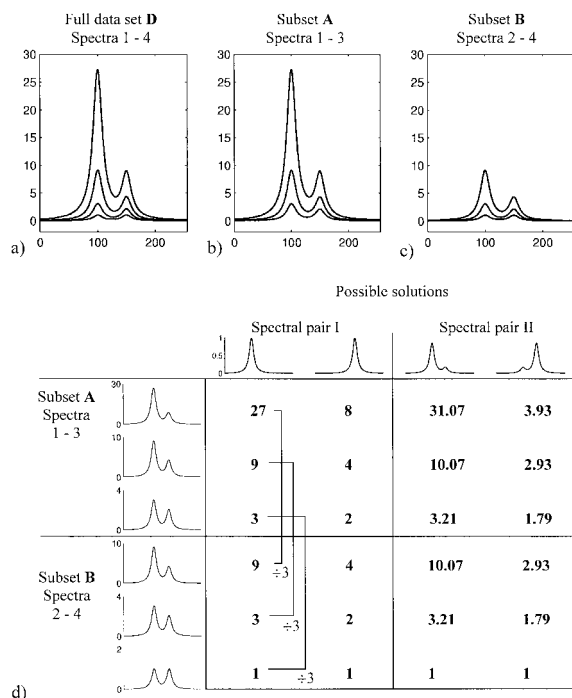


Figure 13 Simulated PGSE NMR data illustrating the principle behind DECRA. (a) The full data set (**D**) showing four mixture spectra comprising the superposition of the spectra of two components having different diffusion coefficients. Data set **D** is split into two other data sets: (b) subset **A**, comprising spectra 1–3 from **D**, and (c) subset **B**, comprising spectra 2–4 from **D**. (d) A grid demonstrating the proportionality. Two possible solutions (spectral pair I and spectral pair II), each having two pure spectra, are shown at the top. The numbers represent the composition of each of the pure spectra that are necessary to reproduce the mixture spectra on the left. For example, 27 times the left pure spectrum in spectral pair I plus 8 times the right pure spectrum in spectral pair II equals spectrum 1 of subset **A**, and so on. Note the different vertical scales. Only one solution can be found given two data sets that are correlated. The fact that the component spectra vary exponentially within the data set satisfies these criteria.

from **A** and spectrum 2 from **B**, spectrum 2 from **A** and spectrum 3 from **B**, and spectrum 3 from **A** and spectrum 4 from **B**), we can see that $27 \div 3 = 9$, $9 \div 3 = 3$, $3 \div 3 = 1$ and $8 \div 2 = 4$, $4 \div 2 = 2$, $2 \div 2 = 1$. The other solution, pair II, does not satisfy this behavior. The proportionality factors are contained within the matrix

$$\beta = \begin{bmatrix} 3 & 0 \\ 0 & 2 \end{bmatrix}.$$

The simple step of splitting the data enables us to satisfy all of the requirements for the GRAM analysis!

An important aspect that should be clear is that the data must be collected with equal q^2 spacing (usually equal g^2 spacing) to satisfy the proportionality requirement (signal $\propto e^{-q^2(\Delta-\delta/3)}$).

Implicit in the algorithm is the discrete exponential behavior. Despite this seemingly strict requirement, DECRA may still be used for polymeric mixtures having distributions in decay rates and it performs amazingly well (20,33). In this case, the precision in the diffusion dimension is reduced because of the nondiscrete nature of the diffusion coefficients, and the resolved diffusion coefficient will be discrete and be most closely related to a number-average diffusion coefficient. DECRA has several advantages including the ability to resolve spectra with low S/N, small differences in diffusion coefficients, and severe spectral overlap. It is a fast method that may be applied to all or part of a data set. Typically, a set of 16 spectra with 32,000 real points each may be fully processed in under 10 s using a typical UNIX-based workstation. *A priori* knowledge of the number of components is necessary. The only user input, in fact, is the number of pure components. Because a direct solution is found, the algorithm is very fast, so many guesses can be made within a short period of time. Generally, if too many pure components are chosen, the extra component will look like noise only or have small peaks that have roughly equal amounts of positive and negative. There is a limit to the number of resolved components; five seems to be a practical maximum (33). There is also a practical limit to the resolution in the diffusion dimension that will depend on the polydispersity of the diffusion coefficient for each component, the S/N, and the general quality of the data. Differences as small as 20% were reported (19). However, this is at least an order of magnitude worse in resolution compared to the simple DOSY approach described earlier. Because exponential processes are prevalent in spectroscopy, DECRA is broadly applicable. Besides PGSE NMR data of small molecules and polymers, DECRA was also applied to MRI (99,100), kinetic (33,101), and solid-state NMR data (39).

Other Approaches

Two other curve resolution approaches are mentioned here, CORE and MCR. They differ significantly from DECRA and DOSY and were shown to produce good results. CORE is a global, two-level, least-squares minimization procedure that fits all of the data to a predetermined model. The model can be based on signal decay as with diffusion or time-resolved fluorescence data or on both the signal increase and decay

as with kinetics. All may be modeled with an expression including a sum of exponential functions. The procedure has the advantage of being able to deal with data that have highly overlapped spectral components and very low S/N. No *a priori* knowledge of the bandshapes is needed. It will be limited, however, in the number of components that may be resolved. It was successfully applied to PGSE NMR data of surfactant mixtures (22), polymer-surfactant mixtures (21,102), time resolved fluorescence (23), kinetics (23), and MRI data (103).

MCR is actually a general term that may refer to a number of analyses. As described in the work by Van Gorkom and Hancewicz (24), MCR refers to an approach that uses principal factor analysis (92) and incorporates alternating least-squares optimization (104) and Varimax rotation (92) in order to generate real chemical factors from abstract factors. MCR in this context produces pure factors and scores and transforms them into physically meaningful spectra and decay rates, respectively.

Considering all of the methods available, it is clear that no one approach will be able to extract all of the information within the data set. Each has its own set of attributes and limitations. All are complimentary and should be used with discretion. The author adopted the practice of using two methods, DECRA and the simplest version of DOSY (i.e., not involving the ILT). The DOSY analysis provides great precision in the diffusion dimension for well-resolved regions of the spectrum, and DECRA provides the ability to examine overlapped regions. These two methods are discussed in the next section through two examples. A comparison is made between the two techniques to highlight their complementary nature and to again stress the importance of data quality.

EXAMPLES

Two mixtures are examined in this section. They are chosen because they represent challenging mixture analyses. The components have diffusion coefficients that are close in magnitude, as well as having portions of high spectral overlap. With these examples, the reader should have a good idea of the ability and limitations of PGSE NMR mixture analysis.

The first to consider is the glucose/sucrose mixture in water with added TSP. Figure 14 shows the DOSY plot of the mixture. The data set, composed of 16 spectra, was Fourier transformed with 16,000 real points. FIDDLE was performed on the data using the TSP resonance as the reference and applying baseline correction. Good separation of water, glucose, and

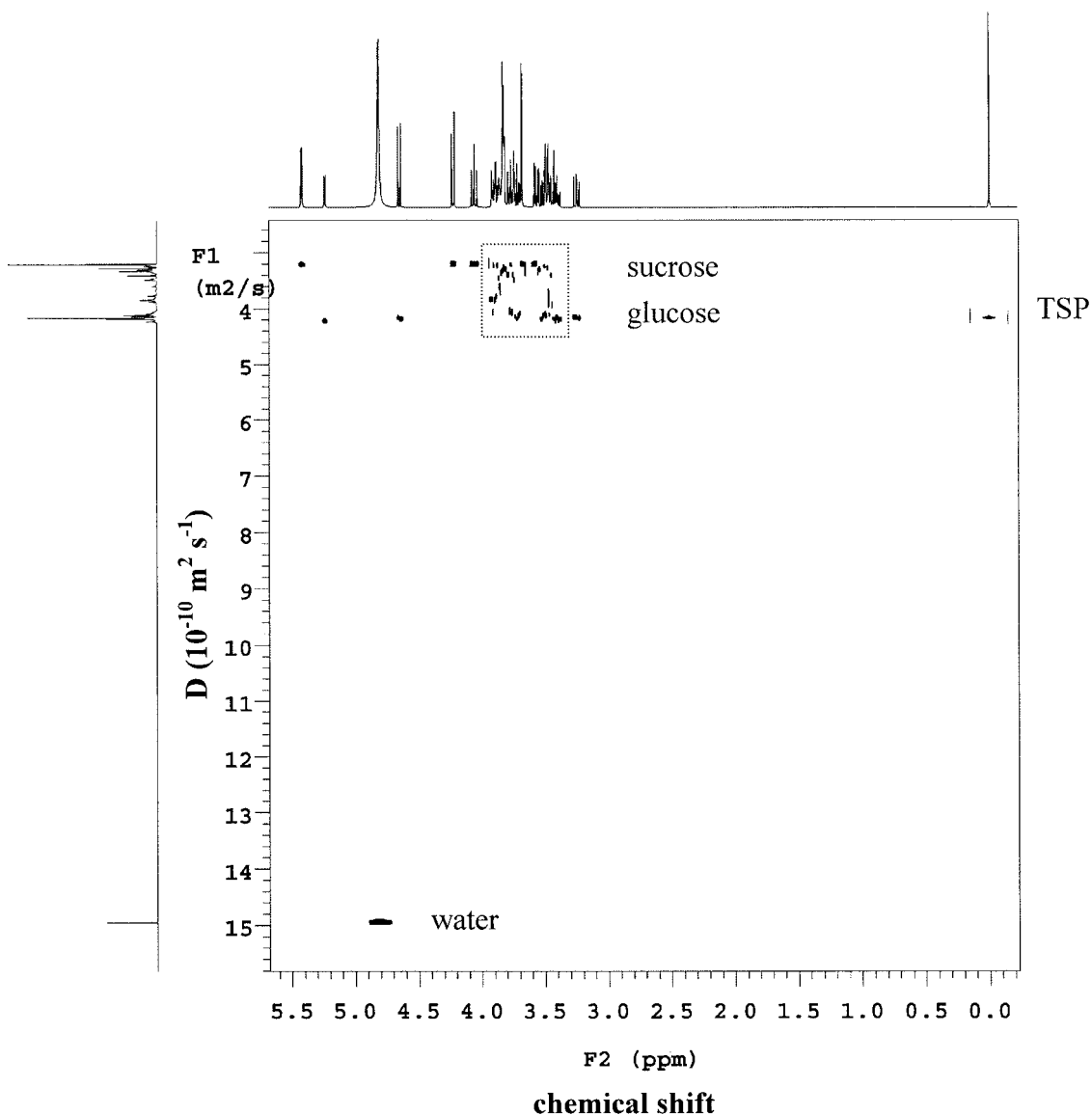


Figure 14 A DOSY plot of the glucose/sucrose solution with TSP at 21°C. Most of the glucose resonances are well separated from the sucrose resonances. The main problem, however, that is typical of this data analysis is indicated with the dotted box. Signal overlap leads to the formation of peaks that are between two components and actually represent the weighted average of the two resonances. Note that TSP and glucose have nearly identical diffusion coefficients. The two peaks on either side of the TSP peak are the ^{13}C satellites.

sucrose is apparent. However, there is a large degree of spectral overlap in the region between 3.3 and 4.0 ppm (indicated with a dotted box). This results in a group of cross peaks in the region between the two extremes that represents weighted averages of the spectral contributions of each component at those frequency values. It is also noted that, although TSP and glucose are different molecules, they have virtually identical diffusion coefficients. One must always be aware of this caveat when using diffusion as a

means to separate mixtures. Better separation may be achieved with the addition of a surfactant, so that not only the size but also the molecular binding plays a role in the measured diffusion coefficient (30).

To better examine the overlapped region, DECRA was used on the same data set shown in Fig. 14, and the results are shown in Figs. 15 and 16. This method resolves three components: water, glucose with TSP, and sucrose. A typical output of the DECRA program installed in VNMR is shown in Fig. 15. At the left of

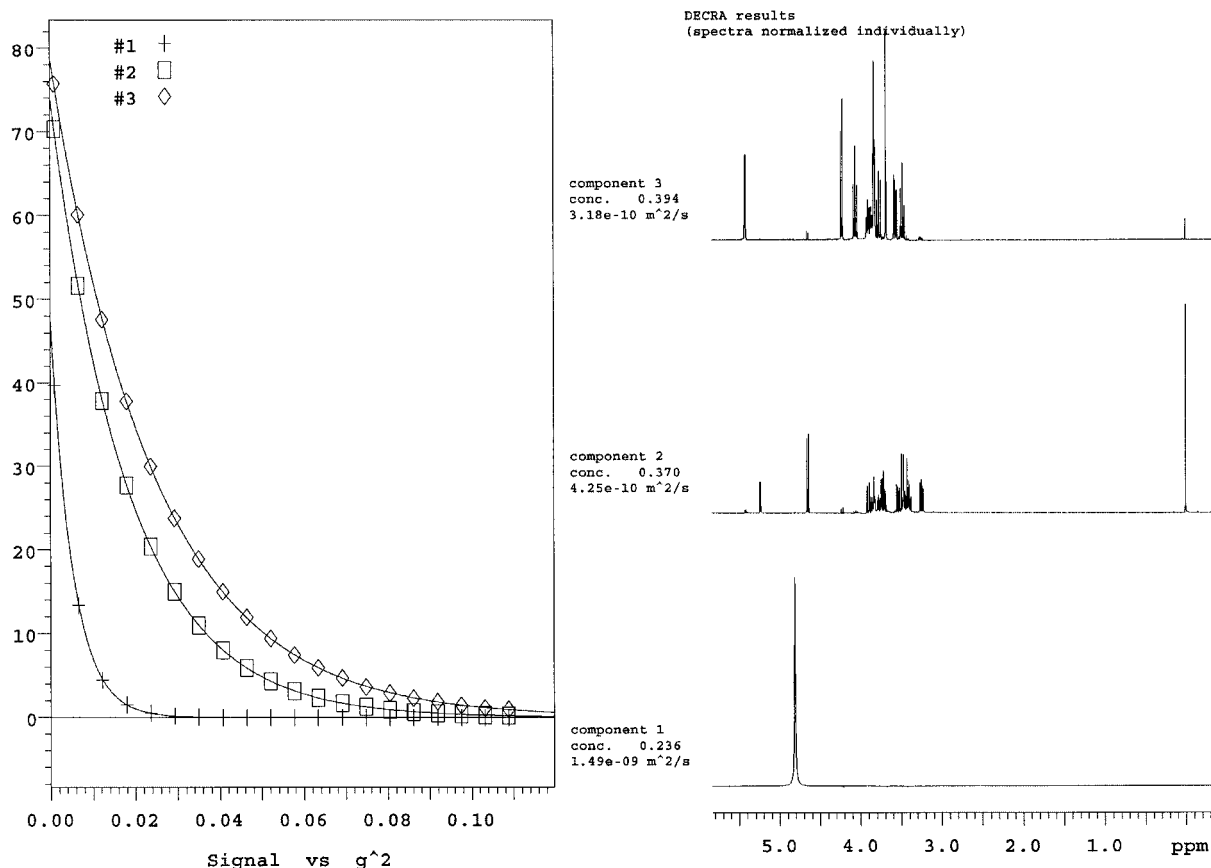


Figure 15 DECRA processing and plots of the same data set used in Fig. 14. Three components are used for the analysis. The plot on the left represents the signal decay of each component within the data set. The spectral plot on the right shows the resolved pure components, along with the calculated diffusion coefficients and concentrations.

the figure is a plot of the concentration profiles for each of the three resolved components in each spectrum analyzed. The concentration refers to the total integrated area of the resolved spectrum. On the right are the resolved spectra, and the extracted diffusion coefficients are listed next to each spectrum and are proportional to the decay rates of the concentration profiles on the left. Also included is the concentration of the spectrum in the mixture calculated for the $g^2 = 0$ case and normalized to a total of 1. As expected, TSP could not be separately resolved and is included in the glucose spectrum. A closer examination of the resolved spectra is included in Fig. 16. The glucose and sucrose spectra resolved in this analysis are directly compared with reference spectra from solutions containing only one component. Despite severe overlap in the region between 3.3 and 4.0 ppm, DECRA does a very good job at fully resolving the pure component spectra.

Problems in the analysis may arise, however, as a result of acquisition artifacts. Figure 16(g,h) is the

result of a DECRA analysis on a data set acquired without slice selection. In this case, because the magnetic field gradient is nonuniform across the excited region, the signal decay for each component is impure, possessing a multiexponential character. This violates the model implicit in DECRA and produces artifacts in the results. Generally, these artifacts are realized as “leakages” of one component into the other. Small glucose resonances are seen in the sucrose spectrum in Fig. 16(h) and vice versa in Fig. 16(g). Interestingly, it was found that the slower moving component has a greater presence in the spectrum of the faster component under these circumstances. This result underscores the importance of pure exponential decay when resolving components having very similar diffusion coefficients.

The results for three different methods of measurement, manual (i.e., one peak at a time), DOSY, and DECRA, are listed in Table 3. No error analysis was performed. Glucose and sucrose have very close diffusion coefficients. If one compares the difference

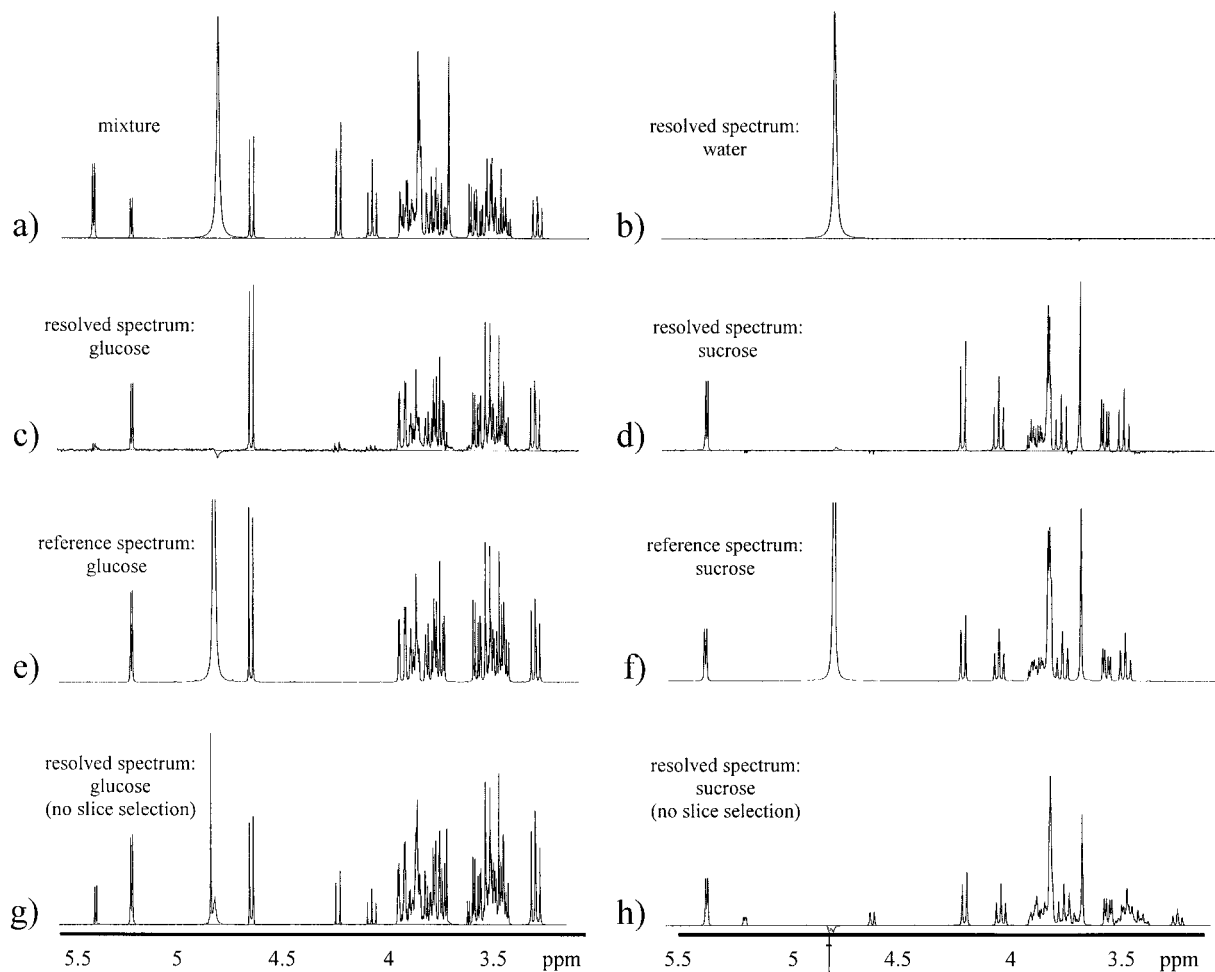


Figure 16 A spectral comparison of the DECRA resolved components and references from the data set shown in Figs. 14 and 15 and from single component solutions, respectively. (a) A mixture spectrum containing all three components (the first spectrum of the PGSE NMR data set). The DECRA resolved (b) water spectrum, (c) glucose spectrum, and (d) sucrose spectrum. Reference spectra for (e) glucose and (f) sucrose. DECRA resolved spectra from a data set acquired without the use of slice selection for (g) glucose and (h) sucrose. Note the large residual signals of other components in each of the resolved spectra in (g) and (h). These are an indication of impure exponential decay and are dramatically reduced with the use of slice selection.

between the two values with the average of the two values, they differ by 29%. If one divides the larger value by the smaller value, they are different by a factor of 1.3. The DECRA analysis cleanly resolved the overlapped regions, despite the close diffusion coefficients. This represents a significant improvement over the DOSY analysis of overlapped regions using SPLMOD or DISCRETE where under only the best circumstances can separation be made with differences better than 67% (or by a factor of 2). The resolution of components with differences as little as 17% was demonstrated by DECRA analysis using a probe with a gradient coil designed to have optimum field uniformity (19).

The second example involves a mixture of three compounds that have similar chemical structures, toluene, diphenylamine, and tri-*p*-tolylphosphine. It is not uncommon to encounter a situation where at least part of the mixture comprises similar compounds. The data set, containing 16 spectra, was Fourier transformed with 16,000 real points. No additional post-processing, besides a linear baseline correction, was used. The DOSY results are in Fig. 17 and the DECRA results are in Fig. 18. Conclusions similar to the first example can be made. The DOSY analysis worked well for the resolved regions and DECRA for the overlapped regions. The aromatic region of the DECRA resolved components is shown in Fig. 19,

Table 3. Diffusion Coefficients ($\times 10^{-10} \text{ m}^2 \text{ s}^{-1}$) Measured at 21°C by Three Methods

	Mixture 1		Mixture 2			
	Glucose	Sucrose	Toluene	Diphenylamine	Tri- <i>p</i> -tolylphosphine	TMS
Manual	4.11	3.10	20.3 ^a (21.6 ^{b,c})	15.8	10.7 (10.6 ^c)	21.6
DOSY	4.20	3.20	21.1 (22.4 ^c)	16.3	10.7 (10.6 ^c)	21.4
DECRA	4.25	3.18	22.6	16.1	10.7	21.3

^a The first 4 spectra only are used in the calculation.

^b The first 10 spectra only are used in the calculation.

^c The window function used for enhancing the spectral resolution.

along with the reference spectra. The purity of the separation is quite good. Table 3 compares the diffusion coefficients obtained from all three methods. It is important to note the differences in the diffusion coefficients of the three components in the mixture with TMS. Whereas in the previous example there was no detectable difference between the diffusion

coefficients for TSP and glucose, in this example there appears to be a measurable difference between TMS and toluene. In the DOSY plot illustrated in Fig. 17, toluene is shown to diffuse slower than TMS. However, an independent experiment with only toluene and TMS in CD_2Cl_2 suggested the opposite was true. The problem lies in the fact that there are no

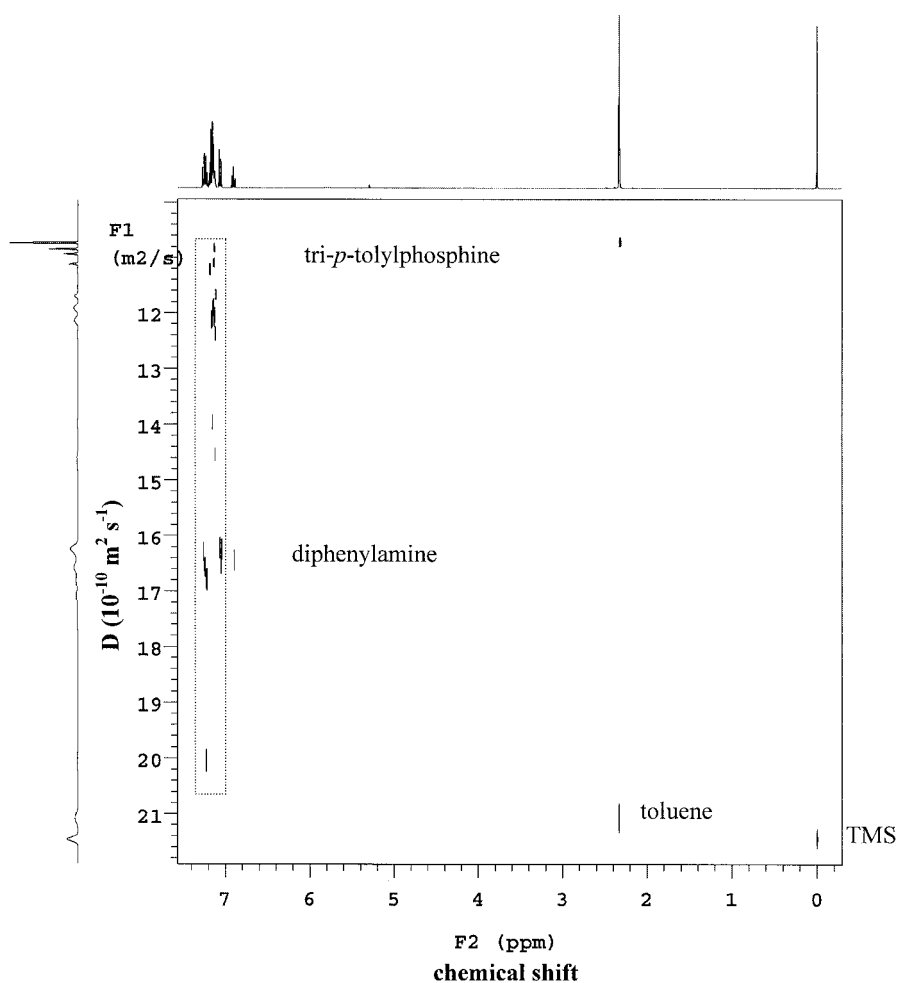


Figure 17 A DOSY plot of the toluene/diphenylamine/tri-*p*-tolylphosphine mixture with TMS at 21°C. Because of severe overlap, the aromatic region is poorly resolved in the diffusion dimension (as indicated with the dotted box). In this case the TMS is resolved from the toluene.

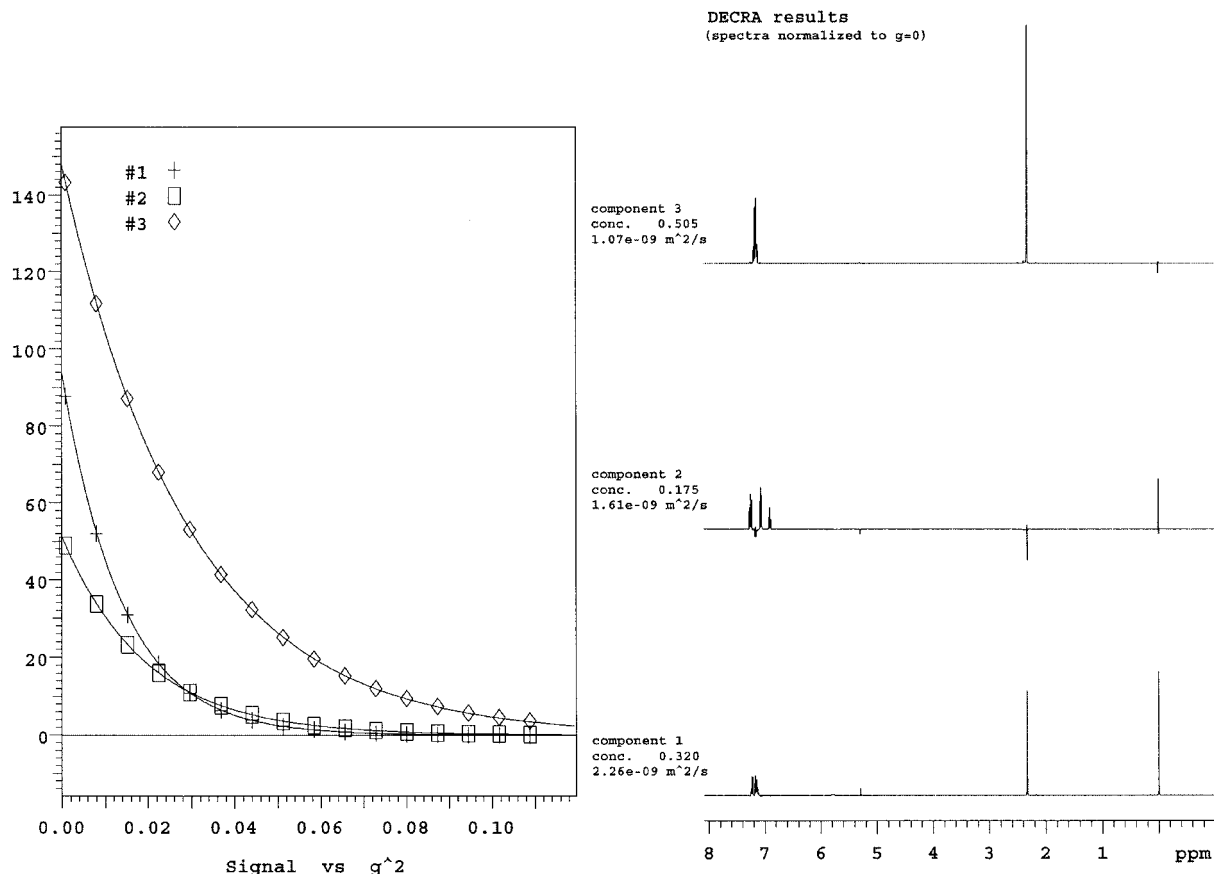


Figure 18 DECRA processing and plots of the same data set used in Fig. 17. Three components are used for the analysis. The aromatic region is well resolved by this method. However, the TMS is not due to the fact that its diffusion coefficient is too close in value to that of the toluene.

toluene resonances that are completely baseline resolved in the three-component mixture. The toluene aromatic resonances are fully overlapped, but the toluene methyl is almost fully resolved from that of the tri-*p*-tolylphosphine. The methyl region is shown in Fig. 20. Figure 20(a) shows the normally processed data where no window function is used. There is a slight overlap between the two resonances as is apparent by the superposition of the DECRA resolved peaks. The threshold used for the DOSY analysis in Fig. 17 includes the overlapped portions. Therefore, the DOSY analysis reports weighted averages for the diffusion coefficients. The problem is more severe for the toluene than the tri-*p*-tolylphosphine because it is the lesser component. The data was subsequently processed with a window function, described in the figure caption and designed to provide an enhanced resolution (at the expense of S/N). Using this window function, the more accurate diffusion coefficients were obtained and are shown in Table 3. Note that although DECRA could not resolve the TMS spec-

trum from the others, it could nonetheless provide the diffusion coefficient when only the TMS region was analyzed.

Our last example is not a mixture analysis but an evaluation of simple polymer solutions. In order to determine the practical limits in using a conventional high resolution gradient probe for measuring diffusion coefficients, a small study was conducted to compare the results of PGSE NMR with DLS on dilute PSS solutions. This problem presents many challenges. The ¹H spectrum of PSS is rather broad owing to the short T_2 relaxation times, which is typical of most polymers. The polymer concentration is low (0.15%, w/w). Finally, the molecular weight is high so the diffusion coefficients are very low. Moreover, the measures put in place to improve the data quality, degrade the S/N at the same time. Figure 21 shows the results of this comparative study. The pulse sequence, egsteSLc, was used. The CLUB-sandwich gradient composite enabled the use of shorter delay times, which allowed for the minimization of signal loss due

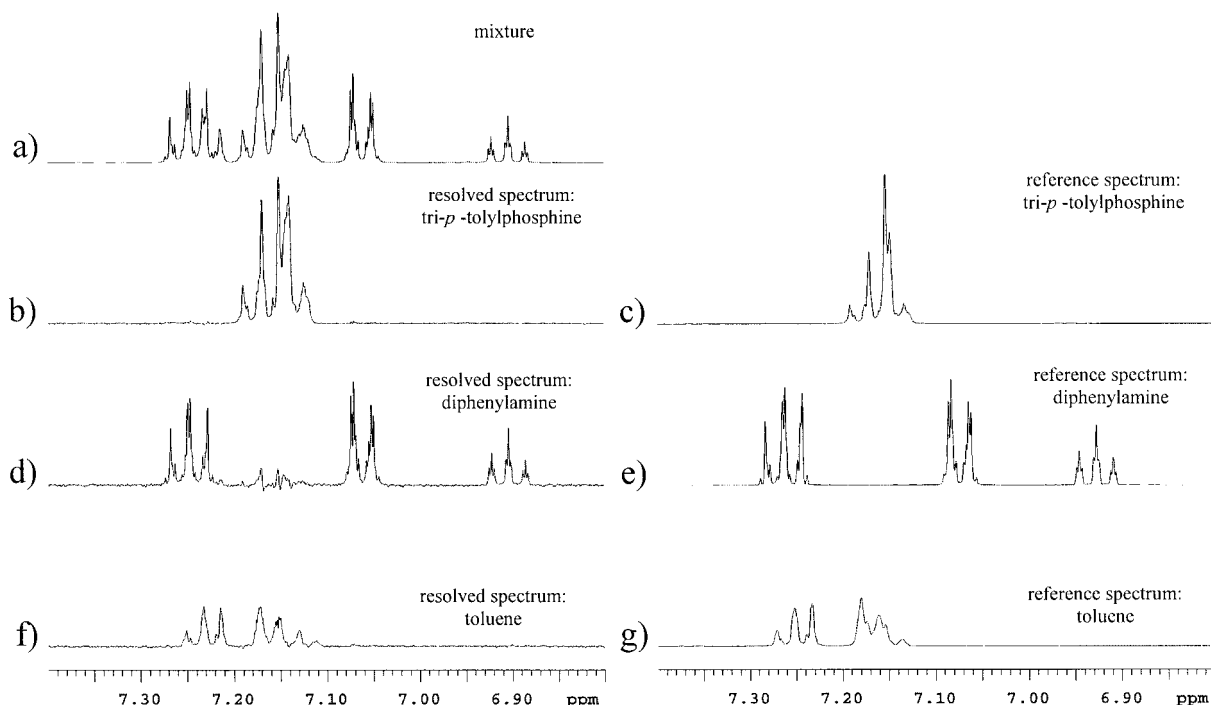


Figure 19 A spectral comparison of the DECRA resolved components and references from the data set shown in Figs. 17 and 18 and from single-component solutions, respectively. Only the aromatic region is used for the analysis. (a) A mixture spectrum containing all three components (the first spectrum of the PGSE NMR data set). (b) The DECRA resolved tri-*p*-tolylphosphine spectrum. (c) A reference tri-*p*-tolylphosphine spectrum. (d) The DECRA resolved diphenylamine spectrum. (e) A reference diphenylamine spectrum. (f) The DECRA resolved toluene spectrum. (g) A reference toluene spectrum.

to T_2 relaxation. Furthermore, longer gradient pulse lengths could be used without increasing the duty cycle beyond a safe point. The highest sample molecular weight in the series that was measurable by PGSE NMR using the probe described in the Experimental section was 350 kDa. The measured diffusion coefficient for this sample was $1.27 \times 10^{-11} \text{ m}^2 \text{ s}^{-1}$, which corresponds to a R_H of 19 nm. The main problem in looking at the higher molecular weight polymers in the series is that the gradient length became too long, and hence the signal loss because of T_2 is too great. To measure lower diffusion coefficients, one simply needs stronger gradients to achieve shorter gradient times. To measure diffusion coefficients for species of lower concentrations, we need a probe that delivers better gradient uniformity (i.e., a larger region of constant gradients), thereby avoiding the need for slice selection. Lower diffusion coefficients and lower concentrations may be achieved with polymers with longer T_2 times and better spectral characteristics such as PEO and poly(dimethylsiloxane).

These examples help to illustrate the benefits of a multiapproach analysis to obtain all of the possi-

ble information. DOSY is a good first analysis because, in the form used here, there is no *a priori* knowledge of the mixture that is necessary for the analysis. It gives a good survey of the components present. The problem is simply spectral overlap. Because this is a common occurrence in mixture spectra, we apply DECRA on the overlapped region(s). Now the main problem is with close differences in the diffusion coefficients (another common occurrence in mixtures). How close can the differences be for DECRA to be effective? This will depend solely upon the quality of the data set. If systematic and random artifacts are both eliminated, gradient field nonuniformity remains as the limiting factor. Because of their distribution of the molecular weight, polymers exhibit a natural multiexponential decay behavior that will inherently limit the analysis. The criteria for determining how much multiexponential character (natural or artificial) is tolerable in the mixture analysis were not rigorously determined. In separate experiments, co-mixtures of toluene/tri-*p*-tolylphosphine and toluene/diphenylamine were examined by DECRA with

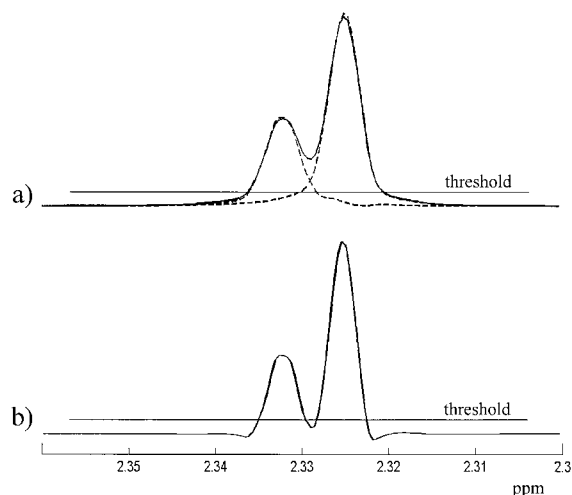


Figure 20 The expansion of the methyl region for the toluene/diphenylamine/tri-*p*-tolylphosphine mixture. (a) (—) The first spectrum of the PGSE NMR data set processed with a line broadening of 0.3 Hz. (---) The DECRA resolved resonances for toluene (2.333 ppm) and tri-*p*-tolylphosphine (2.325 ppm). (b) The first spectrum of the PGSE NMR data set processed with a window function comprising both line broadening and Gaussian functions: $\exp(0.5\pi t) * \exp(-(t/0.9)^2)$, where t is the time value (s). In VNMR, lb = -0.5 and gf = 0.9.

and without slice selection. Good separation was achieved for the toluene/tri-*p*-tolylphosphine mixture without slice selection. The difference between the diffusion coefficients is 70% (or a factor of 2.1). However, slice selection was necessary to achieve good separation of toluene and diphenylamine where the difference is 33% (or a factor of 1.4). Even if slice selection is used, there will still be gradient field nonuniformity to some extent. It then becomes more important to allow for enough signal decay to get good relative differentiation (87). The S/N will also limit these efforts. Differences in diffusion coefficients near 30% seem to be the current practical limit for conventional probe technology. However, with better designed gradient coils, which are optimized for field uniformity, this limit should improve.

Even with the best hardware one has to always bear in mind the main caveat of PGSE NMR mixture analysis: there has to be measurable differences (>1% different) in the component diffusion coefficients. The first example illustrates this point clearly. Three components, α -D-glucopyranose, β -D-glucopyranose, and TSP, have, within experimental precision, the same diffusion coefficient!

CONCLUSIONS

PGSE NMR is a powerful experimental tool for solution mixture analysis. It is a facile first method for identifying components of different molecular size. It requires no physical separation and therefore no special methods development. Although it is not strictly quantitative, it offers a good approximation for solution composition. Many methods for data analysis are available that result in a 2-D display of the diffusion coefficient versus the chemical shift and fall under the general term DOSY. Other methods, including DECRA, CORE, and MCR, focus on resolving spectra under overlapped conditions and were shown to be effective. These methods are complementary and no one data analysis method can extract all of the information from the data set. No matter what analysis approach is used, one must strive to obtain the best possible data quality in order to extract the most information.

There are essentially three problems that lead to spectral artifacts in the data set: eddy currents caused by gradient switching, convection currents caused by temperature gradients, and nonuniform field gradients inherent in the gradient coil design. The adoption of proper pulse sequence elements and appropriate sample configuration will alleviate these problems to a great degree. The most effective solutions to these problems, however, come at the expense of S/N.

With appropriate measures one can resolve components having diffusion coefficients that differ within 2% under conditions without spectral overlap and to within 30% with spectral overlap. Standard

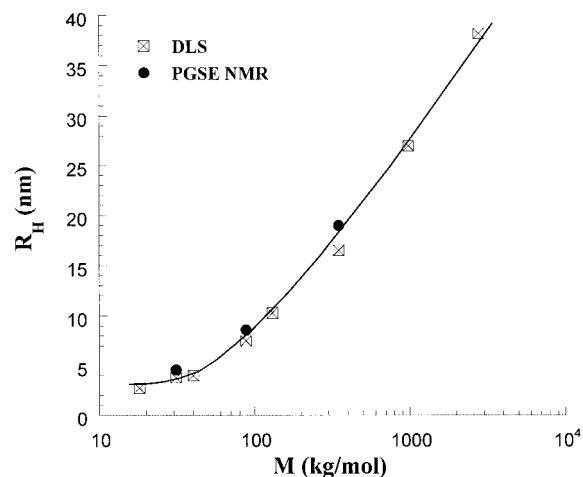


Figure 21 A comparison of the hydrodynamic radius (R_H) for 0.15% (w/w), 0.1N $\text{CH}_3\text{CO}_2\text{Na}$, poly(styrene sulfonate) solutions calculated from DLS and PGSE NMR at 25°C. Equation [1] was used with $\eta = 0.00091$ Pa s.

probe technology with gradient coils achieving a maximum of less than 0.5 T m^{-1} and not strictly designed for PGSE NMR is adequate for mixture analyses of small molecules in nonviscous solvents. More demanding mixture analyses of solutions containing large molecules, components very close in molecular size, or components in low concentrations may require probe hardware optimized for such use, particularly stronger gradient strength and better gradient uniformity.

SOFTWARE

Some of the algorithms and programs described in this report are available and may be obtained from the internet.

1. DECRA (VNMR version only, VNMR user library, password required) available at <http://www.varianinc.com/nmr/apps/usergroup/userlib.html>,
2. CORE (P. Stilbs) available at <http://omega.physchem.kth.se/~peter/>,
3. maximum entropy DOSY processing (GIFA, M.-A. Delsuc) available at <http://www.cbs.univ-montp1.fr/GIFA/welcome.html>, and
4. DISCRETE, SPLMOD, and CONTIN (S. Provencher) available at <http://S-provencher.COM/index.shtml>.

ACKNOWLEDGMENTS

The author is indebted to Willem Windig for his great support and ideas in the development of DECRA. Without his enthusiastic participation, none of this work would have been possible. The author thanks Julia Tan and Etienne Sauvage for performing the DLS experiments on PSSNa solutions. The author also gratefully acknowledges J. Michael Hewitt, Graham Kiddle, Frank Michaels, and William Lenhart for providing valuable input while preparing the manuscript. Finally, the author gratefully appreciates the guidance and detailed comments provided by the referees.

APPENDIX

The MATLAB script for DECRA analysis:

```
function [pspec,diff,a]=
```

```
decre(fname,constant,grad2,spec,startspec,endspec,
      startpoint,endpoint,ncom);

%read in data (phasefile from Varian VNMR software
platform)
fid=fopen(fname,'r','b');
data1=fread(fid,'float');
specsize=round((length(data1)-8-spec*7)/spec);
data=[];
fheader=data1(1:8);
bheader=[];
mask=[zeros(1,startpoint) ones(1,endpoint-start-
point) zeros(1,specsize-endpoint)];
for i=1:1:spec;
    j=(i-1)*specsize+i*7;
    data=[data data1((j+1+8):(j+8+specsize)).
          *mask'];
    bheader=[bheader;data1((j-7+8+1):(j+8))];
end;
fclose(fid);
data=data';
clear data1;

%a constant difference between  $g^2$  is necessary
incr=grad2(2)-grad2(1);

%define two ranges (split the data set in two)
range1=[startspec:endspec-1];
range2=[startspec+1:endspec];

%create a common base for the two data sets using SVD
[vc,sc,uc]=svd(data(range1,:)',0);
sc=sc(1:ncom,1:ncom);
uc=uc(:,1:ncom);
vc=vc(:,1:ncom);

%project the two data sets onto the common base
auv=sc;
buv=uc'*data(range2,:)*vc;

%solve the generalized eigenvalue problem
[v,s]=eig(buv*inv(sc));
ev=diag(s);
[ev,sortindex]=sort(diag(s));
v=v(:,sortindex);

%calculate spectra and concentrations
pspec=pinv(vc*inv(sc)*v);
pint=uc*v;

%scale spectra and concentrations
total=sum(data(range1,:))';
scalefactor=pint\total;
pint=pint*diag(scalefactor);
pspec=diag(1./scalefactor)*pspec;

%calculate proper composition
pint2=pint*diag(ev);
```

```

nrows = size(pint,1);
pintcomb = [pint(1,:);(pint(2:nrows,:)+
    pint2(1:nrows-1,:))/2; pint2(nrows,:)];
b = log(ev)/incr;
diff = -b/constant;
grad21 = grad2(range1);
grad22 = grad2(range2);
grad2comb = [grad21;grad22(nrows)];
for i = 1:length(ev);
    expest0 = exp(grad2comb*b(i));
    a(i) = expest0/pintcomb(:,i);
end;
pspec = diag(a)*pspec;

%rewrite data (phasefile from Varian platform)
data1 = fheader;
for i = 1:1:ncom;
    data1 = [data1;bheader((i-1)*7+1:(i*7));pspec(i,:)]';
end;
pspec = data1;
clear data1;
fid = fopen(fname,'w','b');
fwrite(fid,pspec,'float');
fclose('all');

%end

```

Explanation of Variables in the Matlab Script

<i>pspec</i>	resolved spectra normalized to the $g = 0$ point in the experiment and representative of composition
<i>diff</i>	diffusion coefficients calculated from the eigenvalues
<i>a</i>	relative amounts of each resolved component scaled to $g = 0$
<i>fname</i>	name of file (phasefile in Varian VNMR)
<i>constant</i>	$(\Delta - \delta/3)\gamma^2\delta^2$ (rad s T^{-1}) ²
<i>grad2</i>	g^2 values (T m^{-1}) ²
<i>spec</i>	number of spectra in total
<i>startspec and endspec</i>	range of data to be used
<i>startpoint and endpoint</i>	expansion of data to be used
<i>ncom</i>	number of components chosen
<i>incr</i>	difference in g^2 values (T m^{-1}) ²

REFERENCES

1. Pullen FS, Swanson AG, Newman MJ, Richards DS. 'Online' liquid chromatography/nuclear magnetic res-

onance mass spectrometry—A powerful spectroscopic tool for the analysis of mixtures of pharmaceutical interest. *Rapid Commun Mass Spectrom* 1995; 9:1003–1006.

2. Shockcor JP, Unger SH, Wilson ID, Foxall PJD, Nicholson JK, Lindon JC. Combined HPLC, NMR spectroscopy, and ion-trap mass spectrometry with application to the detection and characterization of xenobiotic and endogenous metabolites in human urine. *Anal Chem* 1996; 68:4431–4435.
3. Clayton E, Preece S, Taylor S, Wilson L, Wright B. The use of LC-NMR-MS in pharmaceutical analysis. *Adv Mass Spectrom* 1998; 14:C104540/1–C104540/10.
4. Sandvoss M, Weltring A, Preiss A, Levsen K, Wuenesch G. Combination of matrix solid-phase dispersion extraction and direct on-line liquid chromatography–nuclear magnetic resonance spectroscopy–tandem mass spectrometry as a new efficient approach for the rapid screening of natural products: Application to the total asterosaponin fraction of the starfish *Asterias rubens*. *J Chromatogr A* 2001; 917:75–86.
5. Spraul M, Braumann U, Godejohann M, Hofmann M. Hyphenated methods in NMR [food studies]. *R Soc Chem* 2001; 262:54–66.
6. Callaghan PT. Principles of nuclear magnetic resonance microscopy. Oxford: Clarendon Press; 1991.
7. Stilbs P. Fourier transform pulsed-gradient spin-echo studies of molecular diffusion. *Prog NMR Spectrosc* 1987; 19:1–45.
8. Price WS. Pulsed-field gradient nuclear magnetic resonance as a tool for studying translational diffusion: Part I. Basic theory. *Concepts Magn Reson* 1997; 9:299–336.
9. Price WS. Pulsed-field gradient nuclear magnetic resonance as a tool for studying translational diffusion: Part II. Experimental aspects. *Concepts Magn Reson* 1997; 9:299–336.
10. Stejskal EO, Tanner JE. Spin diffusion measurements: Spin echoes in the presence of a time-dependent field gradient. *J Chem Phys* 1965; 42:288–292.
11. Tanner JE. The use of the stimulated echo in NMR diffusion studies. *J Chem Phys* 1990; 52:2523–2526.
12. Tanner JE, Stejskal EO. Restricted self-diffusion of protons in colloidal systems by the pulsed-gradient, spin-echo method. *J Chem Phys* 1968; 49:1768–1777.
13. Packer KJ, Rees C. Pulsed NMR studies of restricted diffusion. *J Colloid Interface Sci* 1972; 40:206–218.
14. Stilbs P. Molecular self-diffusion coefficients in Fourier transform nuclear magnetic resonance spectrometric analysis of complex mixtures. *Anal Chem* 1981; 53:2135–2137.
15. Johnson CS Jr. Diffusion ordered nuclear magnetic resonance spectroscopy: principles, applications. *Prog NMR Spectrosc* 1999; 34:203–256.
16. Morris KF, Johnson CS Jr. Diffusion-ordered two-dimensional nuclear magnetic resonance spectroscopy. *J Am Chem Soc* 1992; 114:3139–3141.

17. Morris KF, Johnson CS Jr. Resolution of discrete, continuous molecular size distribution by means of diffusion-ordered 2D NMR. *J Am Chem Soc* 1993; 115:4291–4299.
18. Antalek B, Windig W. Generalized rank annihilation method applied to a single multicomponent pulsed gradient spin echo NMR data set. *J Am Chem Soc* 1996; 118:10331–10332.
19. Windig W, Antalek B. Direct exponential curve resolution algorithm (DECRA): A novel application of the generalized rank annihilation method for a single spectral mixture data set with exponentially decaying contribution profiles. *Chemom Intell Lab Syst* 1997; 37:241–254.
20. Windig W, Antalek B. Resolving nuclear magnetic resonance data of complex mixtures by three-way methods: Examples of chemical solutions and the human brain. *Chemom Intell Lab Syst* 1999; 46:207–219.
21. Stilbs P, Paulsen K, Griffiths PC. Global least-squares analysis of large, correlated spectral data sets: Application to component-resolved FT-PGSE NMR spectroscopy. *J Phys Chem* 1996; 100:8180–8189.
22. Griffiths PC, Stilbs P, Paulsen K, Howe AM, Pitt AR. FT-PGSE NMR study of mixed micellization of an anionic and a sugar-based nonionic surfactant. *J Phys Chem B* 1997; 101:915–918.
23. Stilbs P, Paulsen K. Global least-squares analysis of large, correlated spectral data sets. Application to chemical kinetics and time-resolved fluorescence. *Rev Sci Instrum* 1996; 67:4380–4386.
24. Van Gorkom LCM, Hancewicz TM. Analysis of DOSY and GPC-NMR experiments on polymers by multivariate curve resolution. *J Magn Reson* 1998; 130:125–130.
25. Derrick TS, Larive CK. Use of PFG-NMR for mixture analysis: Measurement of diffusion coefficients of cis and trans isomers of proline-containing peptides. *Appl Spectrosc* 1999; 53:1595–1600.
26. Jayawickrama AD, Larive CK, McCord EF, Roe CD. Polymer additives mixture analysis using pulsed-field gradient NMR spectroscopy. *Magn Reson Chem* 1998; 36:755–760.
27. Kapur GS, Findeisen M, Berger S. Analysis of hydrocarbon mixtures by diffusion-ordered NMR spectroscopy. *Fuel* 2000; 79:1347–1351.
28. Mistry N, Ismail IM, Farrant RD, Liu M, Nicholson JK, Lindon JC. Impurity profiling in bulk pharmaceutical batches using ^{19}F NMR spectroscopy and distinction between monomeric and dimeric impurities by NMR-based diffusion measurements. *J Pharm Biomed Anal* 1999; 19:511–517.
29. Barjat H, Morris GA, Smart S, Swanson AG, Williams SCR. High-resolution diffusion-ordered 2D spectroscopy (HR-DOSY)—A new tool for the analysis of complex mixtures. *J Magn Reson Ser B* 1995; 108:170–172.
30. Morris KF, Stilbs P, Johnson CS Jr. Analysis of mixtures based on molecular size, hydrophobicity by means of diffusion-ordered 2D NMR. *Anal Chem* 1994; 66:211–215.
31. Jerschow A, Müller N. Diffusion-separated nuclear magnetic resonance spectroscopy of polymer mixtures. *Macromolecules* 1998; 31:6573–6578.
32. Griffiths PC, Roe JA, Jenkins RL, Reeve J, Cheung AYW, Hall DG, Pitt AR, Howe AM. Micellization of sodium dodecyl sulfate with a series of nonionic *n*-alkyl malono-bis-*N*-methylglucamides in the presence and absence of gelatin. *Langmuir* 2000; 16:9983–9990.
33. Windig W, Antalek B, Sorriero L, Bijlsma S, Louwense DJ, Smilde A. Applications and new developments of the direct exponential curve resolution algorithm (DECRA). Examples of spectra and magnetic resonance images. *J Chemom* 1999; 13:95–110.
34. Lin M, Shapiro MJ, Wareing JR. Diffusion-edited NMR—Affinity NMR for direct observation of molecular interactions. *J Am Chem Soc* 1997; 119:5249–5250.
35. Chen A, Shapiro MJ. Affinity NMR—A new drug-screening tool that probes ligand–receptor interactions. *Anal Chem* 1999; 71:669–675.
36. Hodge P, Monvisade P, Morris GA, Preece I. A novel NMR method for screening soluble compound libraries. *Chem Commun* 2001; 3:239–240.
37. Lin M, Shapiro MJ. Mixture analysis in combinatorial chemistry. Application of diffusion-resolved NMR spectroscopy. *J Org Chem* 1996; 61:7617–7619.
38. Lin M, Shapiro MJ, Wareing JR. Screening mixtures by affinity NMR. *J Org Chem* 1997; 62:8930–8931.
39. Zumbulyadis N, Antalek B, Windig W, Scaringe RP, Lanzafame AM, Blanton T, Helber M. Elucidation of polymorph mixtures using solid-state ^{13}C CP/MAS NMR spectroscopy and direct exponential curve resolution algorithm. *J Am Chem Soc* 1999; 121:11554–11557.
40. Callaghan PT, Codd SL, Seymour JD. Spatial coherence phenomena arising from translational spin motion in gradient spin echo experiments. *Concepts Magn Reson* 1999; 11:181–202.
41. Hahn EL. Spin echoes. *Phys Rev* 1950; 80:580–594.
42. Carr HY, Purcell EM. Effects of diffusion on free precession in nuclear magnetic resonance experiments. *Phys Rev* 1954; 94:630–638.
43. Morris GA, Barjat H, Horne TJ. Reference deconvolution methods. *Prog Nucl Magn Reson Spectrosc* 1997; 31:197–257.
44. Gurst JE. NMR and the structure of D-glucose. *J Chem Ed* 1991; 68:1003–1004.
45. Jehenson P, Westphal M, Schuff N. Analytical method for the compensation of eddy-current effects induced by pulsed magnetic field gradients in NMR systems. *J Magn Reson* 1990; 90:264–278.
46. Price WS, Kuchel PW. Effect of nonrectangular field gradient pulses in the Stejskal and Tanner (diffusion) pulse sequence. *J Magn Reson* 1991; 94:133–139.

47. Merrill MR. NMR diffusion measurements using a composite gradient PGSE sequence. *J Magn Reson Ser A* 1993; 103:223–225.
48. Wider G, Dötsch V, Wüthrich K. Self-compensating pulsed magnetic-field gradients for short recovery times. *J Magn Reson Ser A* 1994; 108:255–258.
49. Haitao H, Shaka AJ. Composite pulsed gradients with refocused chemical shifts and short recovery time. *J Magn Reson* 1999; 136:54–62.
50. Mandelshtam VA, Haitao H, Shaka AJ. Two-dimensional HSQC NMR spectra obtained using a self-compensating double pulsed field gradient and processed using the filter diagonalization method. *Magn Reson Chem* 1998; 36:S17–S28.
51. Håkansson B, Jönsson B, Linse P, Söderman O. The influence of a nonconstant magnetic-field gradient on PFG NMR diffusion experiments. A Brownian-dynamics computer simulation study. *J Magn Reson* 1997; 124:343–351.
52. Freeman R. Shaped radiofrequency pulses in high resolution NMR. *Prog Nucl Magn Reson Spectrosc* 1998; 32:59–106.
53. Goux WJ, Verkruyse LA, Salter SJ. The impact of Rayleigh–Benard convection on NMR pulsed-field-gradient diffusion measurements. *J Magn Reson* 1990; 88:609–614.
54. Mau X-A, Kohlmann O. Diffusion-broadened velocity spectra of convection in variable-temperature BP-LED experiments. *J Magn Reson* 2001; 150:35–38.
55. Jones DW, Child TF. NMR in flowing systems. *Adv Magn Reson* 1976; 8:123–148.
56. Price WS. NMR imaging. *Annu Rep NMR Spectrosc* 1998; 35:139–216.
57. Callaghan PT, Xia Y. Velocity and diffusion imaging in dynamic NMR microscopy. *J Magn Reson* 1991; 91:326–352.
58. Johnson CS Jr. Electrophoretic NMR. In: Grand DM, Harris RK, editors. *Encyclopedia of NMR*; New York: Wiley; 1996. Vol. 2. p 1886–1895.
59. Jerschow A. Thermal convection currents in NMR: Flow profiles and implications for coherence pathway selection. *J Magn Reson* 2000; 145:121–131.
60. Loening NM, Keeler J. Measurement of convection and temperature profiles in liquid samples. *J Magn Reson* 1999; 139:334–341.
61. Mair RW, Tseng C-H, Wong GP, Cory DG, Walsworth RL. Magnetic resonance imaging of convection in laser-polarized xenon. *Phys Rev E* 2000; 61:2741–2748.
62. Hedin N, Furó I. Temperature imaging by ^1H NMR and suppression of convection in NMR probes. *J Magn Reson* 1998; 131:126–130.
63. Gibbs SJ, Carpenter TA, Hall LD. Magnetic resonance imaging of thermal convection. *J Magn Reson Ser A* 1993; 105:209–214.
64. Lounila J, Oikarinen K, Ingman P, Jokisaari J. Effects of thermal convection on NMR and their elimination by sample rotation. *J Magn Reson Ser A* 1996; 118:50–54.
65. Augé S, Amblard-Blondel B, Delsuc M-A. Investigation of the diffusion measurement using PFG and test of robustness against experimental conditions and parameters. *J Chim Phys* 1999; 96:1559–1565.
66. Zhong F, Ecke R, Steinberg V. Asymmetric modes and the transition to vortex structures in rotating Rayleigh–Bénard convection. *Phys Rev Lett* 1991; 67:2473–2476.
67. Goux WJ, Verkruyse LA, Salter SJ. The impact of Rayleigh–Bernard convection on NMR pulsed-field-gradient diffusion measurements. *J Magn Reson* 1990; 88:609–614.
68. Jerschow A, Müller N. Suppression of convection artifacts in stimulated-echo diffusion experiments. Double-stimulated-echo experiments. *J Magn Reson* 1997; 125:372–375.
69. Jerschow A, Müller N. Convection compensation in gradient enhanced nuclear magnetic resonance spectroscopy. *J Magn Reson* 1998; 132:13–18.
70. Sørland GH, Seland JG, Krane J, Anthonsen HK. Improved convection compensating pulsed field gradient spin-echo and stimulated echo methods. *J Magn Reson* 2000; 142:323–325.
71. Wu D, Chen A, Johnson CS Jr. An improved diffusion-ordered spectroscopy experiment incorporating bipolar gradient pulses. *J Magn Reson Ser A* 1995; 115:260–264.
72. Tillet ML, Lu-Yun L, Norwood TJ. Practical aspects of the measurement of the diffusion of proteins in aqueous solution. *J Magn Reson* 1998; 133:379–384.
73. Pelta MD, Barjat H, Morris GA, Davis AL, Hammond SJ. Pulse sequences for high-resolution diffusion-ordered spectroscopy (HR-DOSY). *Magn Reson Chem* 1998; 36:706–714.
74. Altieri AS, Hinton DP, Byrd RA. Association of biomolecular systems via pulsed field gradient NMR self-diffusion measurements. *J Am Chem Soc* 1995; 117:7566–7567.
75. Price WS, Hayamizu K, Ide H, Arata Y. Strategies for diagnosing and alleviating artifactual attenuation associated with large gradient pulses in PGSE NMR diffusion measurements. *J Magn Reson* 1999; 139:205–212.
76. Pescher LJC, Bouwstra JA, de Bleyser J, Junginger HE, Leyte JC. Cross-relaxation in pulsed-field-gradient stimulated-echo measurements on water in a macromolecular matrix. *J Magn Reson Ser B* 1996; 110:150–157.
77. Chen A, Shapiro MJ. Nuclear Overhauser effect on diffusion measurements. *J Am Chem Soc* 1999; 121:5338–5339.
78. Chen A, Johnson CS Jr, Lin M, Shapiro MJ. Chemical exchange in diffusion NMR experiments. *J Am Chem Soc* 1998; 120:9094–9095.
79. Longworth LG. The mutual diffusion of light and heavy water. *J Phys Chem* 1960; 64:1914–1917.

80. Holz M, Heil SR, Sacco A. Temperature-dependent self-diffusion coefficients of water and six selected molecular liquids for calibration in accurate ^1H NMR PFG measurements. *Phys Chem Chem Phys* 2000; 2:4740–4742.
81. Chari K, Antalek B, Minter J. Diffusion and scaling behavior of polymer–surfactant aggregates. *Phys Rev Lett* 1995; 74:3624–3627.
82. Callaghan PT, Pinder DN. Influence of multiple length scales on the behavior of polymer self-diffusion in the semidilute regime. *Macromolecules* 1984; 17:431–437.
83. Lamanna R, Delmelle M, Cannistraro S. Role of hydrogen-bond cooperativity and free-volume fluctuations in the non-Arrhenius behavior of water self-diffusion: A continuity-of-states model. *Phys Rev E* 1994; 49:2841–2850.
84. Mills R. Self-diffusion in normal and heavy water in the range 1–45 degrees. *J Phys Chem* 1973; 77:685–688.
85. Waggoner RA, Blum FD, Lang JC. Diffusion in aqueous solutions of poly(ethylene glycol) at low concentrations. *Macromolecules* 1995; 28:2658–2664.
86. Damberg P, Jarvet J, Gräslund A. Accurate measurement of translational diffusion coefficients: A practical method to account for nonlinear gradients. *J Magn Reson* 2001; 148:343–348.
87. Istratov AA, Vyvenko OF. Exponential analysis in physical phenomena. *Rev Sci Instrum* 1999; 70:1233–1257.
88. Provencher SW. An eigenfunction expansion method for the analysis of exponential decay curves. *J Chem Phys* 1976; 64:2772–2777.
89. Wijnaendts van Resandt RW, Vogel RH, Provencher SW. Double beam fluorescence spectrometer with subnanosecond resolution: Application to aqueous tryptophan. *Rev Sci Instrum* 1982; 53:1392–1397.
90. Provencher SW. CONTIN: A general purpose constrained regularization program for inverting noisy linear algebraic and integral equations. *Comput Phys Commun* 1982; 27:229–242.
91. Delsuc MA, Malliavin, TE. Maximum entropy processing of DOSY NMR spectra. *Anal Chem* 1998; 70:2146–2148.
92. Malinowski ER, Howery DG. *Factor analysis in chemistry*. New York: Wiley–Interscience; 1991.
93. Kubista M. A new method for the analysis of correlated data using Procrustes rotation which is suitable for spectral analysis. *Chemom Intell Lab Syst* 1990; 7:273–279.
94. Scarminio I, Kubista M. Analysis of correlated spectral data. *Anal Chem* 1993; 65:409–416.
95. Booksh KS, Kowalski BR. Comments on data analysis (datan) algorithm and rank annihilation factor analysis for the analysis of correlated spectral data. *J Chemom* 1994; 8:287–292.
96. Sanchez E, Kowalski BR. Generalized rank annihilation factor analysis. *Anal Chem* 1986; 58:496–499.
97. Wilson BE, Sanchez E, Kowalski BR. An improved algorithm for the generalized rank annihilation method. *J Chemom* 1989; 3:493–498.
98. Schulze D, Stilbs P. Analysis of multicomponent FT-PGSE experiments by multivariate statistical methods applied to the complete bandshapes. *J Magn Reson Ser A* 1993; 105:54–58.
99. Windig W, Hornak JP, Antalek B. Multivariate image analysis of magnetic resonance images with the direct exponential curve resolution algorithm (DECRA). Part 1: Algorithm and model study. *J Magn Reson* 1998; 132:298–306.
100. Antalek B, Hornak JP, Windig W. Multivariate image analysis of magnetic resonance images with the direct exponential curve resolution algorithm (DECRA). Part 2: Application to human brain images. *J Magn Reson* 1998; 132:307–315.
101. Windig W, Antalek B, Robbins MJ, Zumbulyadis N, Heckler CE. Applications of the direct exponential curve resolution algorithm (DECRA) to solid state nuclear magnetic resonance and mid-infrared spectra. *J Chemom* 2000; 14:213–227.
102. Griffiths PC, Abbott RJ, Stilbs P, Howe AM. Segregation of mixed micelles in the presence of polymers. *Chem Commun* 1998; 1:53–54.
103. Stilbs P. Component separation in NMR imaging and multidimensional spectroscopy through global least-squares analysis, based on prior knowledge. *J Magn Reson* 1998; 241:236–241.
104. Tauler R, Barcelo D. Multivariate curve resolution applied to liquid chromatography–diode array detection. *Trends Anal Chem* 1993; 12:319–327.

BIOGRAPHY



Brian Antalek received his M.S. degree in materials science and engineering from the Rochester Institute of Technology in 1991 under the supervision of J. P. Hornak. His research involved using MRI techniques to study the diffusion of water within materials including gelatin, plaster, and balsa wood. In 1991 he joined the Eastman Kodak Company as a Research Scientist, where his efforts focus on developing magnetic resonance techniques to study problems associated with traditional photographic products and product manufacturing. In particular, he specializes in the application of PGSE NMR to the study of dynamics in colloidal and polymeric systems.